The Hash Function JH [1]

16 January, 2011

Hongjun Wu [2,3]

wuhongjun@gmail.com

[1]The design of JH is tweaked in this report. The round number of JH is changed from 35.5 to 42. This new version may be referred to as JH42 so as to distinguish it from the original design.

[2]Institute for Infocomm Research, Singapore

[3]Nanyang Technological University, Singapore

Contents

1 Introduction

This document specifies four hash algorithms – JH-224, JH-256, JH-384, and JH-512. These algorithms are efficient in hardware since they are built on simple components. They are also efficient in software with SIMD (128-bit SSE and 256-bit AVX) instructions since the simple components can be computed in parallel and thus suitable for bit-slice implementation.

In the design of JH, we propose a new compression function structure to construct a compression function from a large block cipher with constant key. We also generalize the AES [9] design methodology to high dimensions so that a large block cipher can be constructed from small components easily. With the new compression function structure and the generalized AES design methodology, the security of the JH compression function with respect to differential cryptanalysis [4] can be analyzed relatively easily.

The JH hash functions are efficient in software. With bit-slice implementation using SSE2, the speed of JH is about 19.6 cycles/byte on the Intel Core 2 T6600 microprocessor running 64-bit operating system with Intel C++ compiler (about 23.3 cycles/byte for 32-bit operating system).

The memory required for the hardware implementation of JH hash functions is 1536 bits (including the 512-bit message block). With 256 additional memory bits, the round constants of JH can be generated on the fly. JH-224, JH-256, JH-384 and JH-512 share the same compression function, so it is very efficient to implement these four hash algorithms together in hardware.

JH is strong in security. Each message block is 64 bytes. A message block passes through the 42-round compression function that involves 10752 4×4-bit Sboxes. We found that a differential trail in a compression function involves more than 700 active Sboxes. The large number of active Sboxes ensures that JH is strong against differential attack.

This document is organized as follows. The specifications of JH are given in Sect. 3, 4, 5 and 6. The bit-slice implementation of JH is given in Sect. 7. The variants of JH are given in Sect. 8. Section 9 gives the security analysis of JH. The performance of JH is described in Sect. 10. The design rationale and advantage are given in Sect. 11 and Sect. 12, respectively. Sect. 13 concludes this document.

2 The Compression Function Structure and the Generalized AES Design Methodology

Two techniques are used in the design of JH. We proposed a new compression function structure to construct a compression function from a block cipher with constant key; and we used the generalized AES design methodology to design large block ciphers (efficient in hardware and software) from small components.

2.1 A new compression function structure

JH compression function is constructed from a bijective function (a block cipher with constant key). The compression function structure is given in Fig. 1. The block size of the block cipher is $2m$ bits. In the compression function, the $2m$-bit hash value $H^{(i-1)}$ and the m-bit message block $M^{(i)}$ are compressed into the $2m$-bit $H^{(i)}$. Message digest size is at most m bits.

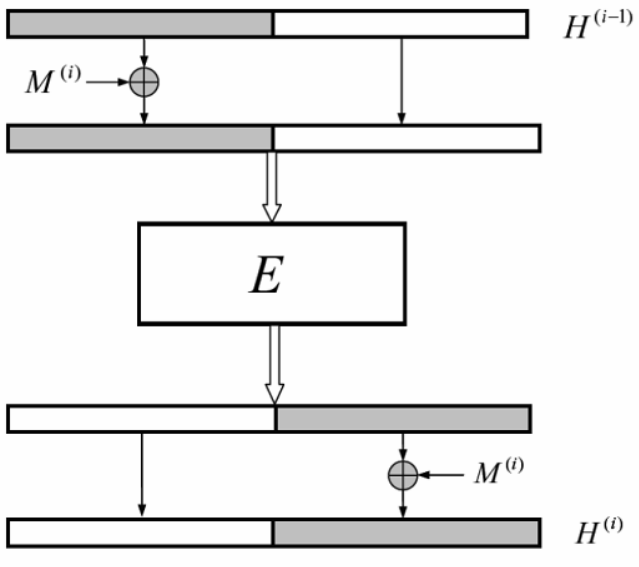

Figure 1: The JH compression function structure

The above compression function structure is simple and efficient. With the key of block cipher being set to constant (permutation), no extra variables are introduced into the middle of the compression function, so it is much easier to analyze the security of this compression function with respect to differential attack (similar feature has appeared in the previous Sponge structure [2]). Without truncating the block cipher output, this structure is quite efficient.

With respect to differential cryptanalysis, we notice that the security evaluation cost of permutation is the lowest; while that of Davies-Meyer structure [27] is very high. Matyas-Meyer-Oseas (MMO) structure [17] is easier to evaluate than Davies-Meyer structure, but its key schedule does not contribute to the differential propagation when only one active compression function is involved in a collision attack. If MMO structure is improved so that its key schedule can always contribute to differential propagation, the improved structure would be similar to sponge structure. If the permutation output in a sponge structure is not truncated so as to improve the computational efficiency, we obtain the JH compression function structure.

2.2 The generalized AES design methodology

AES uses the substitution-permutation network (SPN) with the input as a two-dimensional array. A Maximum Distance Separable (MDS) code is applied to the columns in the even rounds (considering the first round as the zero-th round), and the MDS code is applied to the rows in the odd rounds. Because of the row rotations in AES, the round functions in AES are identical (i.e. there are only mixcolumn operations in AES).

We generalize the AES design to high dimensions so that a large block cipher can be easily constructed from small components. In the generalized AES design methodology, the input bits are divided into $\prod_{i=0}^{d-1} \alpha_i$ ($\alpha_i \geq 2$) elements, and these elements form a d-dimensional array. In the linear layer of the r-th round, an MDS code is applied along the $(r \bmod d)$-th dimension. We believe that the generalized AES design methodology is probably the simplest approach to design an efficient large block cipher from small components.

Here is an example. If we extend AES to three (or four) dimensions, we obtain a block cipher with 512-bit (or 2048-bit) block size immediately. We need to point out that Rijndael with 192-bit and 256-bit block sizes are not based on the generalized AES design since MDS code is not applied to the dimension with 6 (192-bit block size) or 8 (256-bit block size) elements. CS block cipher [22] is based on the generalized AES design with three dimensions, but CS cipher is only efficient on 8-bit platforms.

We use the eight-dimensional generalized AES design to construct the block cipher in JH. The 1024 input bits to the block cipher are divided into 256 4-bit elements, and these elements form an eight-dimensional array. The constant round keys are generated using a six-dimensional block cipher.

For hardware implementation, the round functions of the JH block cipher are identical (using techniques similar to the AES row rotations); for fast software implementation, we use seven different round functions so as to use bit-slice implementation that exploits the power of 128-bit SIMD instructions. The JH block cipher combines the best features of AES (SPN and MDS code) and Serpent (SPN and bit-slice implementation) [1].

3 Definitions

3.1 Notations

The following notations are used in the JH specifications.

Word	A group of bits.
A^i	The i^{th} bit in the word A. An m-bit word A is represented as $A = A^0 \,\|\, A^1 \,\|\, A^2 \,\|\, \cdots \,\|\, A^{m-1}$.

3.2 Parameters

The following parameters are used in the JH specifications.

$C_r^{(d)}$	The round constant words used in function E_d with $0 \leq r \leq 6 \times (d-1)$. Each $C_r^{(d)}$ is a 2^d-bit constant word.
d	The dimension of a block of bits. A d-dimensional block consists of 2^d 4-bit elements.
h	Number of bits in a hash value. $h = 1024$.
$H^{(i)}$	The i^{th} hash value, with a size of h bits. $H^{(0)}$ is the initial hash value; $H^{(N)}$ is the final hash value and is truncated to generate the message digest.
$H^{(i),j}$	The j^{th} bit of the i^{th} hash value, where $H^{(i)} = H^{(i),0} \| H^{(i),1} \| \cdots \| M^{(i),h-1}$.
ℓ	Length of the message, M, in bits.
m	Number of bits in a message block $M^{(i)}$. $m = 512$.
M	Message to be hashed.
$M^{(i)}$	Message block i, with a size of m bits.
$M^{(i),j}$	The j^{th} bit of the i^{th} message block, i.e., $M^{(i)} = M^{(i),0} \| M^{(i),1} \| \cdots \| M^{(i),m-1}$.
N	Number of blocks in the padded message.

3.3 Operations

The following operations are used in the JH specifications.

&	Bitwise AND operation.
$\|$	Bitwise OR ("inclusive–OR") operation.
$\oplus$	Bitwise XOR ("exclusive–OR") operation.
$\neg$	Bitwise complement operation.
$\|\|$	Concatenation operation.

4 Functions

The following functions are used in the JH specifications.

4.1 S-boxes

S_0 and S_1 are the 4×4-bit S-boxes being used in JH. Instead of being simply xored to the input, every round constant bit selects which Sboxes are used (similar to Lucifer [12]) so as to increase the overall algebraic complexity. The logic gates for implementing these two Sboxes are given in Sect. 7.2.1.

x	0	1	2	3	4	5	6	7	8	9	10	11	12	13	14	15
$S_0(x)$	9	0	4	11	13	12	3	15	1	10	2	6	7	5	8	14
$S_1(x)$	3	12	6	13	5	7	1	9	15	2	0	4	11	10	14	8

4.2 Linear transformation L

The linear transformation L implements a (4, 2, 3) Maximum Distance Separable (MDS) code over $GF(2^4)$. Here the multiplication in $GF(2^4)$ is defined as the multiplication of binary polynomials modulo the irreducible polynomial $x^4 + x + 1$. Denote this multiplication as '$\bullet$' . Let A, B, C and D denote 4-bit words. L transforms (A, B) into (C, D) as

$$(C\,, D) = L(A\,, B) = (5\bullet A + 2\bullet B\,,\; 2\bullet A + B)\,.$$

More specifically, the bit-wise computation of L is given as follows. Let A, B, C and D denote 4-bit words, i.e., $A = A^0 \,\|\, A^1 \,\|\, A^2 \,\|\, A^3$, $B = B^0 \,\|\, B^1 \,\|\, B^2 \,\|\, B^3$, $C = C^0 \,\|\, C^1 \,\|\, C^2 \,\|\, C^3$, and $D = D^0 \,\|\, D^1 \,\|\, D^2 \,\|\, D^3$. In polynomial form, A is represented as $A^0x^3 + A^1x^2 + A^2x + A^3$; $2 \bullet A$ is given as $A^1x^3 + A^2x^2 + (A^0 + A^3)x + A^0$. The function $(C, D) = L(A, B)$ is computed as:

$$\begin{aligned}
D^0 &= B^0 \oplus A^1\,; & D^1 &= B^1 \oplus A^2\,;\\
D^2 &= B^2 \oplus A^3 \oplus A^0\,; & D^3 &= B^3 \oplus A^0\,;\\
C^0 &= A^0 \oplus D^1\,; & C^1 &= A^1 \oplus D^2\,;\\
C^2 &= A^2 \oplus D^3 \oplus D^0\,; & C^3 &= A^3 \oplus D^0\,.
\end{aligned}$$

4.3 Permutation P_d

P_d is a simple permutation on 2^d elements. It is similar to the row rotations in AES so as to obtain identical round functions for hardware implementation. It is constructed from π_d, P'_d and ϕ_d. Denote 2^d input elements as $A = (a_0, a_1, \cdots, a_{2^d-1})$, and 2^d output elements as $B = (b_0, b_1, \cdots, b_{2^d-1})$.

4.3.1 Permutation π_d

π_d operates on 2^d elements. The computation of $B = \pi_d(A)$ is as follows:

$$\begin{aligned}
b_{4i+0} &= a_{4i+0} \quad \text{for } i = 0 \text{ to } 2^{d-2} - 1\,;\\
b_{4i+1} &= a_{4i+1} \quad \text{for } i = 0 \text{ to } 2^{d-2} - 1\,;\\
b_{4i+2} &= a_{4i+3} \quad \text{for } i = 0 \text{ to } 2^{d-2} - 1\,;\\
b_{4i+3} &= a_{4i+2} \quad \text{for } i = 0 \text{ to } 2^{d-2} - 1\,;
\end{aligned}$$

The permutation π_4 is illustrated in Fig. 2.

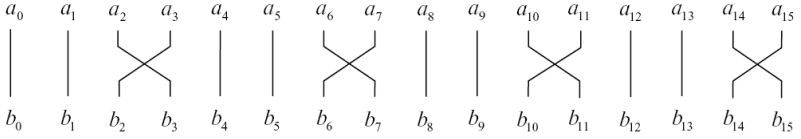

Figure 2: The permutation π_4

4.3.2 Permutation P'_d

P'_d is a permutation on 2^d elements. The computation of $B = P'_d(A)$ is given as follows:

$$\begin{aligned} b_i &= a_{2i} \quad \text{for } i = 0 \text{ to } 2^{d-1} - 1\,; \\ b_{i+2^{d-1}} &= a_{2i+1} \text{ for } i = 0 \text{ to } 2^{d-1} - 1\,; \end{aligned}$$

The permutation P'_4 is illustrated in Fig. 3.

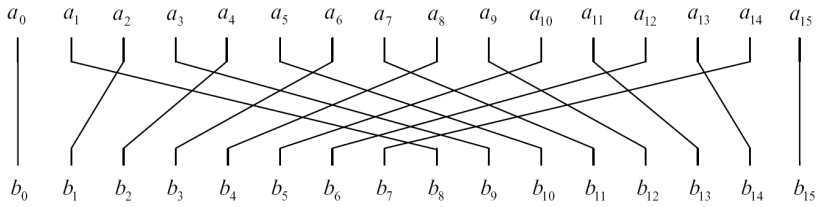

Figure 3: The permutation P'_4

4.3.3 Permutation ϕ_d

ϕ_d is a permutation on 2^d elements. The computation of $B = \phi_d(A)$ is given as follows:

$$\begin{aligned} b_i &= a_i \quad \text{for } i = 0 \text{ to } 2^{d-1} - 1\,; \\ b_{2i+0} &= a_{2i+1} \quad \text{for } i = 2^{d-2} \text{ to } 2^{d-1} - 1\,; \\ b_{2i+1} &= a_{2i+0} \quad \text{for } i = 2^{d-2} \text{ to } 2^{d-1} - 1\,; \end{aligned}$$

The permutation ϕ_4 is illustrated in Fig. 4.

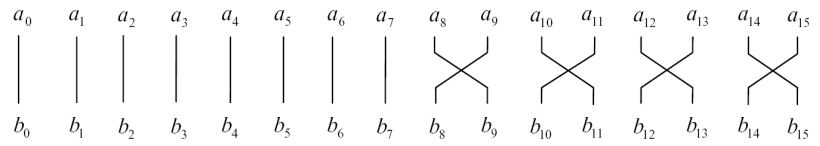

Figure 4: The permutation ϕ_4

4.3.4 Permutation P_d

P_d is the composition of π_d, P'_d and ϕ_d:

$$P_d = \phi_d \circ P'_d \circ \pi_d$$

The permutation P_4 is illustrated in Fig. 5.

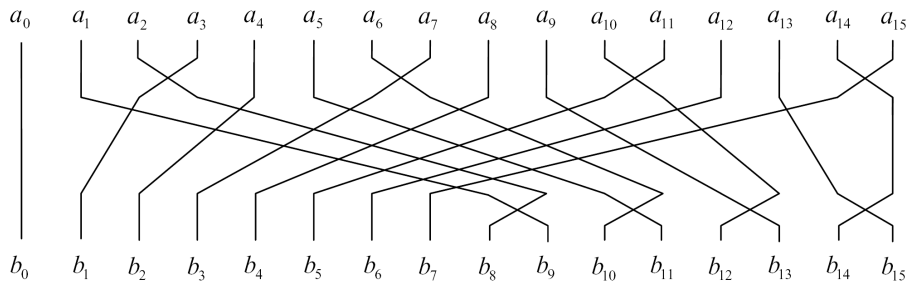

Figure 5: The permutation P_4

4.4 Round function R_d

The round function R_d implements the generalized AES design methodology illustrated in Sect. 2.2. It consists of three layers: the Sbox layer, the linear transformation layer and the permutation layer P_d (similar to the three layers in the round function of AES: Sbox layer, linear transformation and row rotations). The input and output sizes of R_d are 2^{d+2} bits. The 2^{d+2}-bit input word is denoted as $A = (a_0 \,\|\, a_1 \,\|\, \cdots \,\|\, a_{2^d-1})$, where each a_i represents a 4-bit word. The 2^{d+2}-bit output word is denoted as $B = (b_0 \,\|\, b_1 \,\|\, \cdots \,\|\, b_{2^d-1})$, where each b_i represents a 4-bit word. The 2^d-bit round constant of the r-th round is denoted as $C_r^{(d)} = C_r^{(d),0} \| C_r^{(d),1} \cdots \| C_r^{(d),2^d-1}$. Let each v_i and w_i $(0 \le i \le 2^d - 1)$ represent a 4-bit word. The computation of $B = R_d(A, C_r^{(d)})$ is given as follows:

1. for $i = 0$ to $2^d - 1$,
   {
   if $C_r^{(d),i} = 0$, then $v_i = S_0(a_i)$;
   if $C_r^{(d),i} = 1$, then $v_i = S_1(a_i)$;
   }
2. $(w_{2i}, w_{2i+1}) = L(v_{2i}, v_{2i+1})$ for $0 \le i \le 2^{d-1} - 1$;
3. $(b_0, b_1, \cdots, b_{2^d-1}) = P_d(w_0, w_1, \cdots, w_{2^d-1})$;

Two rounds of R_4 are illustrated in Fig. 6.

4.5 Bijective function E_d

E_d is based on the d-dimensional generalized AES design methodology. It applies SPN and MDS code to a d-dimensional array with the MDS code being applied along the $(r \bmod d)$-th dimension in the r-th round. It is constructed from $6(d-1)$ rounds of R_d. The 2^{d+2}-bit input and output are

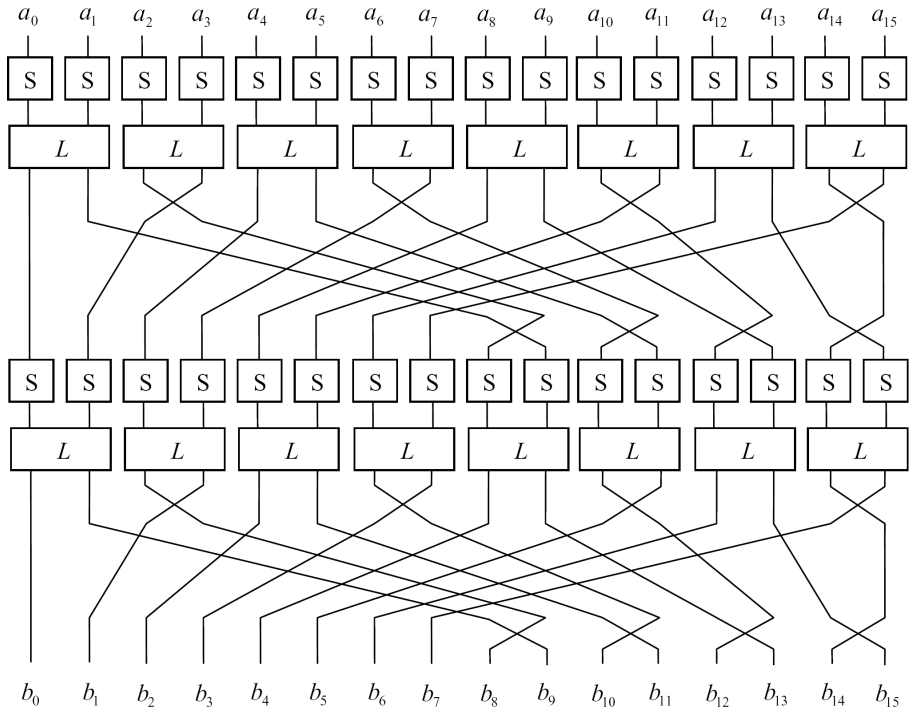

Figure 6: Two rounds of R_4 (round constant bits not shown)

denoted as A and B, respectively. Let each Q_r denote a 2^{d+2}-bit word for $0 \leq r \leq 6(d-1)$, and $Q_r = (q_{r,0} \,\|\, q_{r,1} \,\|\, \cdots \,\|\, q_{r,2^d-1})$, where each $q_{r,i}$ denotes a 4-bit word. The computation of $B = E_d(A)$ is given as follows:

1. grouping the bits of A into 2^d 4-bit elements to obtain Q_0 ;
2. for $r = 0$ to $6(d-1)-1$, $Q_{r+1} = R_d(Q_r, C_r^{(d)})$;
3. de-grouping the 2^d 4-bit elements in $Q_{6(d-1)}$ to obtain B ;

The grouping of bits into 4-bit elements in the first step and the de-grouping in the last step are designed to achieve efficient bit-slice software implementation. The grouping in the first step is given as follows (as shown in Fig. 7):

for $i = 0$ to $2^{d-1} - 1$,
{
$$q_{0,2i} = A^i \| A^{i+2^d} \| A^{i+2\cdot 2^d} \| A^{i+3\cdot 2^d} ;$$
$$q_{0,2i+1} = A^{i+2^{d-1}} \| A^{i+2^{d-1}+2^d} \| A^{i+2^{d-1}+2\cdot 2^d} \| A^{i+2^{d-1}+3\cdot 2^d} ;$$
}

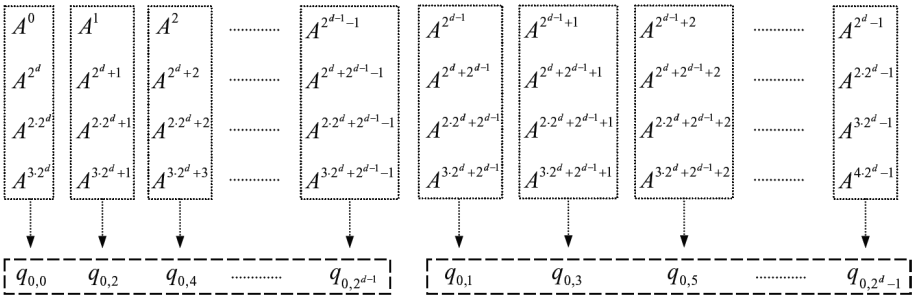

Figure 7: The grouping in function E_d

The de-grouping in the last step is given as follows (as shown in Fig. 8):

for $i = 0$ to $2^{d-1} - 1$,
{
$$B^i \| B^{i+2^d} \| B^{i+2\cdot 2^d} \| B^{i+3\cdot 2^d} = q_{6(d-1),2i} ;$$
$$B^{i+2^{d-1}} \| B^{i+2^{d-1}+2^d} \| B^{i+2^{d-1}+2\cdot 2^d} \| B^{i+2^{d-1}+3\cdot 2^d} = q_{6(d-1),2i+1} ;$$
}

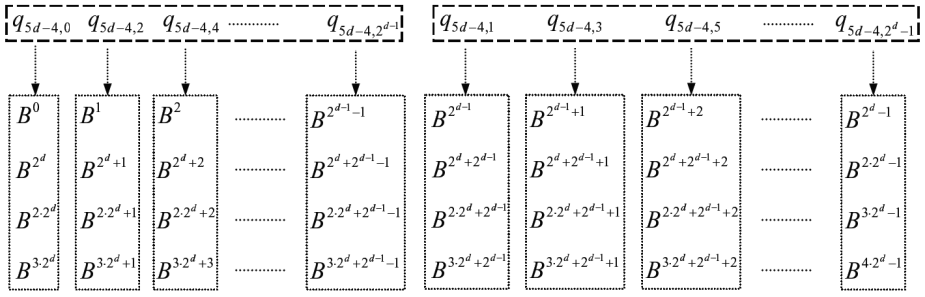

Figure 8: The de-grouping in function E_d

The round constants of E_d are given in Sect. 4.6.

4.6 Round constants of E_d

The round constants $C_r^{(d)}$ for E_d are generated from the round function R_{d-2} (with all the round constants of R_{d-2} being set as 0). Each $C_r^{(d)}$ is a 2^d-bit word. They are generated as follows:

$$C_0^{(d)} \text{ is the integer part of } (\sqrt{2}-1) \times 2^{2^d};$$
$$C_r^{(d)} = R_{d-2}(C_{r-1}^{(d)}, 0) \text{ for } 1 \le r < 6(d-1)\,.$$

The values of $C_r^{(8)}$ $(0 \le r \le 41)$ are given in Appendix A.1.

5 Compression Function F_d

Compression function F_d is constructed from the function E_d. F_d compresses the 2^{d+1}-bit message block $M^{(i)}$ and 2^{d+2}-bit $H^{(i-1)}$ into the 2^{d+2}-bit $H^{(i)}$:

$$H^{(i)} = F_d(H^{(i-1)}, M^{(i)})\,.$$

The construction of F_d is shown in Fig. 9. According to the definition of E_d, the input to every first-layer Sbox would be affected by two message bits; and the output from every last-layer Sbox would be XORed with two message bits.

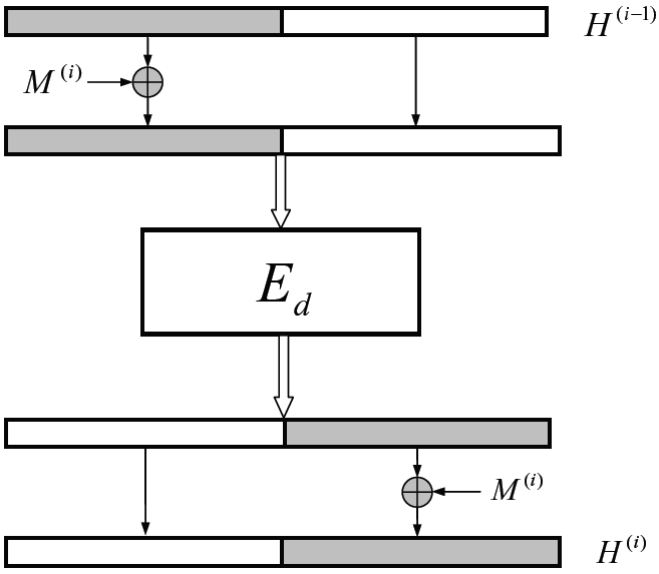

Figure 9: The compression function F_d

5.1 F_8

F_8 is the compression function used in hash function JH. F_8 compresses the 512-bit message block $M^{(i)}$ and 1024-bit $H^{(i-1)}$ into the 1024-bit $H^{(i)}$. F_8 is constructed from E_8. Let A, B denote two 1024-bit words. The computation of $H^{(i)} = F_8(H^{(i-1)}, M^{(i)})$ is given as:

1. $A^j = H^{(i-1),j} \oplus M^{(i),j}$ for $0 \leq j \leq 511$;
   $A^j = H^{(i-1),j}$ for $512 \leq j \leq 1023$;
2. $B = E_8(A)$;
3. $H^{(i),j} = B^j$ for $0 \leq j \leq 511$;
   $H^{(i),j} = B^j \oplus M^{(i),j-512}$ for $512 \leq j \leq 1023$;

6 JH Hash Algorithms

Hash function JH consists of five steps: padding the message M (Sect. 6.1), parsing the padded message into message blocks (Sect. 6.2), setting the initial hash value $H^{(0)}$ (Sect. 6.3), computing the final hash value $H^{(N)}$ (Sect. 6.4), and generating the message digest by truncating $H^{(N)}$ (Sect. 6.5).

6.1 Padding the message

The message M is padded to be a multiple of 512 bits. Suppose that the length of the message M is ℓ bits. Append the bit "1" to the end of the message, followed by $384 - 1 + (-\ell \bmod 512)$ zero bits (for $\ell \bmod 512 = 0, 1, 2, \cdots, 510, 511$, the number of zero bits being padded are $383, 894, 893, \cdots, 385, 384$, respectively), then append the 128-bit block that is equal to the number ℓ expressed using a binary representation in big endian form. Thus at least 512 additional bits are padded to the message M.

6.2 Parsing the padded message

After a message has been padded, it is parsed into N 512-bit blocks, $M^{(1)}$, $M^{(2)}$, ..., $M^{(N)}$. The 512-bit message block is expressed as four 128-bit words. The first 128 bits of message block i are denoted as $M_0^{(i)}$, the next 128 bits are $M_1^{(i)}$, and so on up to $M_3^{(i)}$.

6.3 Setting the initial hash value $H^{(0)}$

The initial hash value $H^{(0)}$ is set depending on the message digest size. The first two bytes of $H^{(-1)}$ are set as the message digest size, and the rest bytes of $H^{(-1)}$ are set as 0. Set $M^{(0)}$ as 0. Then $H^{(0)} = F_8(H^{(-1)}, M^{(0)})$.

More specifically, the value of $H_0^{(-1),0} \| H_0^{(-1),1} \| \cdots \| H_0^{(-1),15}$ is $0x00E0$, $0x0100$, $0x0180$, $0x0200$ for JH-224, JH-256, JH-384 and JH-512, respectively. Let $H^{(-1),j} = 0$ for $16 \leq j \leq 1023$. Set the 512-bit $M^{(0)}$ as 0. The 1024-bit initial hash value $H^{(0)}$ is computed as

$$H^{(0)} = F_8(H^{(-1)}, M^{(0)}) \ .$$

6.4 Computing the final hash value $H^{(N)}$

The compression function F_8 is applied to generate $H^{(N)}$ by compressing $M^{(1)}$, $M^{(2)}$, ..., $M^{(N)}$ iteratively. The 1024-bit final hash value $H^{(N)}$ is computed as follows:

$$\begin{aligned} &\text{for } i = 1 \text{ to } N, \\ &\qquad H^{(i)} = F_8(H^{(i-1)}, M^{(i)}) \, ; \end{aligned}$$

6.5 Generating the message digest

The message digest is generated by truncating $H^{(N)}$.

6.5.1 JH-224

The last 224 bits of $H^{(N)}$ are given as the message digest of JH-224:

$$H^{(N),800} \| H^{(N),801} \| \cdots \| H^{(N),1023} \ .$$

6.5.2 JH-256

The last 256 bits of $H^{(N)}$ are given as the message digest of JH-256:

$$H^{(N),768} \| H^{(N),769} \| \cdots \| H^{(N),1023} \ .$$

6.5.3 JH-384

The last 384 bits of $H^{(N)}$ are given as the message digest of JH-384:

$$H^{(N),640} \| H^{(N),641} \| \cdots \| H^{(N),1023} \ .$$

6.5.4 JH-512

The last 512 bits of $H^{(N)}$ are given as the message digest of JH-512:

$$H^{(N),512} \| H^{(N),513} \| \cdots \| H^{(N),1023} \ .$$

7 Bit-Slice Implementation of JH

The description of JH given in Sect. 4 and Sect. 5 are suitable for efficient hardware implementation. In this section, we illustrate the bit-slice implementation of JH. Seven different round functions are used in the bit-slice implementation of F_8 in JH (the hardware description of F_8 uses identical round function description). The details of developing the bit-slice implementation are given in Appendix B.

7.1 Bit-slice parameters

The following additional parameters are used in the bit-slice implementation of JH.

$C_r'^{(8)}$	The round constant words used in the bit-slice implementation of E_d with $0 \leq r \leq 41$. Each $C_r'^{(8)}$ is a 256-bit constant word.
$C_{r,even}'^{(8)}$	Even bits of $C_r'^{(8)}$. $C_{r,even}'^{(8)} = C_r'^{(8),0} \parallel C_r'^{(8),2} \parallel C_r'^{(8),4} \parallel \cdots \parallel C_r'^{(8),254}$. Each $C_{r,even}'^{(8)}$ is a 128-bit constant word.
$C_{r,odd}'^{(8)}$	Odd bits of $C_r'^{(8)}$. $C_{r,odd}'^{(8)} = C_r'^{(8),1} \parallel C_r'^{(8),3} \parallel C_r'^{(8),5} \parallel \cdots \parallel C_r'^{(8),255}$. Each $C_{r,odd}'^{(8)}$ is a 128-bit constant word.
$H_j^{(i)}$	The j^{th} 128-bit word of the i^{th} hash value. $H_0^{(i)}$ is the left-most 128-bit word of hash value $H^{(i)}$.
$M_j^{(i)}$	The j^{th} 128-bit word of the i^{th} message block. $M_0^{(i)}$ is the left-most word of message block $M^{(i)}$.

7.2 Bit-slice functions

The following functions are used in the bit-slice implementation of JH.

7.2.1 Sboxes

S^{bitsli} implements both S_0 and S_1 in the bit-slice implementation of JH. Let each x_i $(0 \leq i \leq 3)$ denote a 128-bit word. Let c denote a 128-bit constant word, t denote a 128-bit temporary word. $(x_0, x_1, x_2, x_3) = S^{bitsli}(x_0, x_1, x_2, x_3, c)$ is computed in the following 11 steps (x_3 are the least significant bits):

1. $x_3 = \neg x_3$;
2. $x_0 = x_0 \oplus (c \,\&\, (\neg x_2))$;
3. $t = c \oplus (x_0 \,\&\, x_1)$;
4. $x_0 = x_0 \oplus (x_2 \,\&\, x_3)$;
5. $x_3 = x_3 \oplus ((\neg x_1) \,\&\, x_2)$;
6. $x_1 = x_1 \oplus (x_0 \,\&\, x_2)$;
7. $x_2 = x_2 \oplus (x_0 \,\&\, (\neg x_3))$;
8. $x_0 = x_0 \oplus (x_1 | x_3)$;
9. $x_3 = x_3 \oplus (x_1 \,\&\, x_2)$;
10. $x_1 = x_1 \oplus (t \,\&\, x_0)$;
11. $x_2 = x_2 \oplus t$;

7.2.2 Linear Transform

L^{bitsli} implements the linear transform in the bit-slice implementation of JH. Let each a_i and b_i $(0 \leq i \leq 7)$ denotes a 128-bit word. $(b_0, b_1, \cdots, b_7) = L^{bitsli}(a_0, a_1, \cdots, a_7)$ is computed as follows:

$$\begin{aligned} b_4 &= a_4 \oplus a_1\,; & b_5 &= a_5 \oplus a_2\,; \\ b_6 &= a_6 \oplus a_3 \oplus a_0\,; & b_7 &= a_7 \oplus a_0\,; \\ b_0 &= a_0 \oplus b_5\,; & b_1 &= a_1 \oplus b_6\,; \\ b_2 &= a_2 \oplus b_7 \oplus b_4\,; & b_3 &= a_3 \oplus b_4\,. \end{aligned}$$

7.2.3 Permutation ω

Permutation $\omega(A, n)$ swaps the bits in a 128-bit word A. For example, $\omega(A, 1)$ swaps A^{2i} with A^{2i+1}. Let n be a power of 2. Let $A = A^0 \| A^1 \| \cdots \| A^{127}$. $\omega(A, n)$ is computed as follows:

for $i = 0$ to $(128/2n - 1)$,
  SWAP($A^{2\times i\times n} \| A^{2\times i\times n+1} \| \cdots \| A^{2\times i\times n+n-1}$,
  $A^{2\times i\times n+n} \| A^{2\times i\times n+n+1} \| \cdots \| A^{2\times i\times n+2n-1}$);

7.3 Pseudo code for the bit-slice implementation of E_8

Denote the 1024-bit input to E_8 as eight words $x_0||x_1||\cdots||x_7$, where each x_i denotes a 128-bit word. Divide the 256-bit round constant $C_r'^{(8)}$ into 128-bit $C_{r,even}'^{(8)}$ and 128-bit $C_{r,odd}'^{(8)}$. The values of $C_{r,even}'^{(8)}$ and $C_{r,odd}'^{(8)}$ are given in Appendix A.2.

The computation of $E_8(x_0||x_1||\cdots||x_7)$ is given in the following pseudo code:

for $r = 0$ to 41 ,
{
  /* Sbox layer */
  $(x_0, x_2, x_4, x_6) = S^{bitsli}(x_0, x_2, x_4, x_6, C_{r,even}'^{(8)})$;
  $(x_1, x_3, x_5, x_7) = S^{bitsli}(x_1, x_3, x_5, x_7, C_{r,odd}'^{(8)})$;
  /* MDS transformation */
  $(x_0, x_2, x_4, x_6, x_1, x_3, x_5, x_7) = L^{bitsli}(x_0, x_2, x_4, x_6, x_1, x_3, x_5, x_7)$;
  /* Swapping */
  $x_1 = \omega(x_1,\, 2^{r \bmod 7})$;
  $x_3 = \omega(x_3,\, 2^{r \bmod 7})$;
  $x_5 = \omega(x_5,\, 2^{r \bmod 7})$;
  $x_7 = \omega(x_7,\, 2^{r \bmod 7})$;
}

7.4 Bit-slice implementation of F_8

F_8 compresses the 512-bit message block $M^{(i)}$ and 1024-bit $H^{(i-1)}$ into the 1024-bit $H^{(i)}$, where $M^{(i)} = M_0^{(i)} \| M_1^{(i)} \| M_2^{(i)} \| M_3^{(i)}$, $H^{(i)} = H_0^{(i)} \| H_1^{(i)} \| \cdots \| H_7^{(i)}$. The computation of $H^{(i)} = F_8(H^{(i-1)}, M^{(i)})$ is given as:

1. $A_j = H_j^{(i-1)} \oplus M_j^{(i)}$ for $0 \le j \le 3$;
   $A_j = H_j^{(i-1)}$ for $4 \le j \le 7$;
2. $B = E_8(A)$;
3. $H_j^{(i)} = B_j$ for $0 \le j \le 3$;
   $H_j^{(i)} = B_j \oplus M_{j-4}^{(i)}$ for $4 \le j \le 7$;

Note that in function $E(A)$, each word is 128-bit, so JH can be computed efficiently using the 128-bit SSE instructions. For a 128-bit word x, $\omega(x, n)$ can be implemented using two AND operations (AND with a constant to extract the bits to be swapped), two shift operations and one OR operations (note that the shift operations would be affected by the endianess of the SSE2 register). In addition, $\omega(x, 32)$ and $\omega(x, 64)$ can be implemented with one SSE2 shuffle operation.

In function $E(A)$, 256 Sboxes are computed in parallel, so JH can be computed efficiently using the 256-bit AVX instructions (the AVX instructions are now available on the Intel Sandy Bridge processors since January 2011).

8 Variants of JH

The design of JH hash algorithms implies several variants by varying the parameter d or by replacing P_d with P'_d in round function R_d.

8.1 Varying the parameter d

The compression function F_d gives several compression functions by varying the parameter d.

F_6. $d = 6$. With 256-bit hash value and 128-bit message block, this compression function is extremely hardware efficient. A tiny hash function using this compression function can achieve about 128-bit security level for collision resistance, preimage resistance and second preimage resistance for 256-bit message digest size. Note that this tiny hash function is only to

meet the collision resistance requirement.

F_7. $d = 7$. With 512-bit block size and 256-bit message block size, this compression function is used to generate 256-bit message digest size. The memory required is half of that of F_8, and it achieves 128-bit security for collision resistance, 256-bit security for preimage resistance.

F_9. $d = 9$. With 2048-bit block size, this compression function is extremely efficient on the future microprocessors that support shift and binary operations over 256-bit registers.

8.2 Replacing P_d with P'_d

Replacing permutation P_d with P'_d in round function R_d, and changing the round number $6(d-1)$ to $6d$ in E_d, we can obtain another family of compression functions. This family of compression functions are slightly simpler in hardware, but its bit-slice implementation requires twice amount of shift operations as that required in F_d. A few variants can be obtained by varying the value of d.

9 Security Analysis of JH

The security of JH hash algorithms are stated below ($\bar{l}$ denotes the number of message blocks, the length of a message is less than 2^{128} bits):

	collision	second-preimage	preimage
JH-224	2^{112}	2^{224}	2^{224}
JH-256	2^{128}	2^{256}	2^{256}
JH-384	2^{192}	2^{384}	2^{384}
JH-512	2^{256}	$2^{512-\log_2\bar{l}}$	2^{512}

Note that the second-preimage resistance of JH-512 is affected by herding attack [14]. The reason is that the collision resistance of JH-512 is stated as 2^{256}, although the size of the hash value $H^{(i)}$ is 1024 bits. However, JH-512 would not be affected by herding attack if birthday attack is applied to find collisions in herding attack.

9.1 Overview of collision attacks on JH

In the security analysis of JH, we mainly consider the differential and truncated differential collision attacks since they are the main threats to JH. In particular, we found that truncated differential collision attack is the most powerful attack on JH. Our current analysis shows that the complexity of

truncated differential collision attack on JH is more than 2^{512} (with the assumption that message modification can affect up to 16 rounds), much larger than the complexity of brute force (2^{256}).

In the differential and truncated differential collision attacks, we consider mainly the differential probability after message modification. We consider message modification as the technique that can be used to obtain a desired differential pair after t rounds with **average** complexity of about one compression function operation (we emphasize the word 'average' here so as to include the effect of generating multiple differential pairs, such as neutral-bit technique [5] and boomerang technique [13]). **After message modification, if the differential probability is less than $2^{-n/2}$ (n is the message digest size), then unlikely the differential collision attack on JH can be successful**. It is the guideline being used in our security analysis of JH.

From the above guideline, we notice that there are two challenges in the differential and truncated differential collision attacks. One challenge is to determine the maximum number of rounds that can be effectively bypassed using message modification. In the collision attacks on JH, we assume that 16 rounds may be effectively bypassed using message modification. Another challenge is to find the differential paths with the largest probability. In the collision attacks on JH, we use the methods illustrated in Sect. 9.2 to find the differential paths with the largest probability.

9.2 Methods used in the differential analysis of JH

Differential cryptanalysis was originally developed to attack block ciphers [4]. Differential attack was found to be important in analyzing the collision resistance of hash functions, and it has been applied to break MD4, MD5, SHA-0 and SHA-1 [11, 8, 5, 6, 23, 24, 25, 26].

JH was designed in such a way that its differential property can be analyzed relatively easily. We used the following methods in the differential analysis of JH. (These methods have been mentioned in the original JH report. Here we illustrate these methods in detail.)

9.2.1 Method 1: Brute force search on E_d with small values of d

For $d \in \{2, 3, 4\}$, we exhaustively searched for the minimum number of active Sboxes. The minimum number of active Sboxes for $2d + 1$ Sbox layers is 10, 20, 38 for $d = 2, 3, 4$, respectively. To reduce the complexity of brute force, early-stop method is needed (for a differential characteristics, once the number of active Sboxes within certain rounds becomes too large, stop extending that differential path).

The analysis of E_2 is very similar to the analysis of AES since both analysis involve a two-dimensional array. An example of the differential

path with minimum number of active Sboxes for 7 rounds of E_3 is given below (there are seven rows, and each row involves 8 Sboxes in one round. The '*' signs indicate the positions of the active Sboxes):

```
*0*00000
**00**00
*0*00000
**00**00
*0*00000
**00**00
*0*00000
```

An example of the differential path with minimum number of active Sboxes for 9 rounds of E_4 is given below:

```
*0*0000000000000
**000000**000000
*000*00000000000
*0*00000*0*00000
**00**00**00**00
*0*0*0*000000000
****0000****0000
**00**0000000000
*0*0000000000000
```

The results from brute force analysis are important since we can find out when the minimum number of active Sboxes would appear. We made the following observations from those results:

1. To minimize the number of active Sboxes, the positions of active elements in each round need to satisfy certain symmetric property so as to maximize difference cancelation in the subsequent rounds (it also implies that the number of active elements in each round needs to be the power of 2 for achieving the minimum number of active Sboxes).

2. The number of active of Sboxes is reduced when two active Sboxes before the linear transformation L result in only one active element after L. With this observation, the cost of security analysis can be reduced significantly.

3. For the position(s) of the active element(s) after L, we can select them to form symmetric pattern so as to enable difference cancelation in the subsequent rounds. This observation is also very userful for reducing the security evaluation cost.

From the above observations, we are able to find the minimum number of active Sboxes in JH efficiently.

9.2.2 Method 2: Using a simplified E_d in the analysis

We notice that replacing P_d with P'_d in E_d would not affect the minimum number of active Sboxes (since it is equivalent to modifying the MDS code in E_d). We denote this simplified function with P'_d as E'_d. (The reason that we use E_d instead of E'_d in JH is to reduce the number of shift operations in software implementation.)

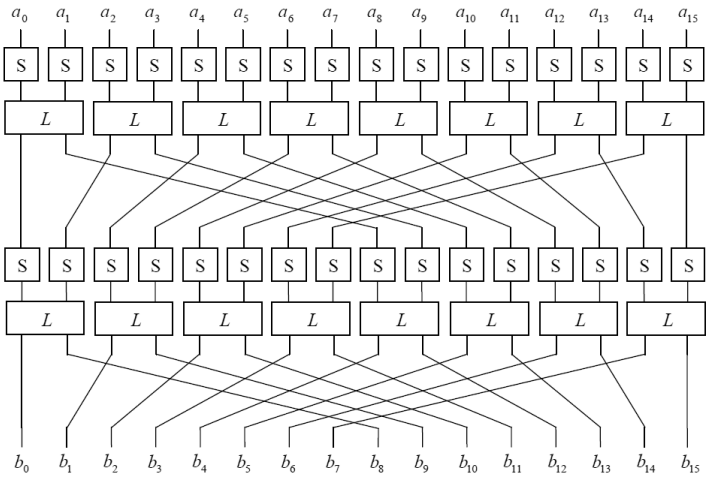

Figure 10: Two rounds in E'_d (round constants are not shown)

E'_d can be described in an alternative form (the form that can be used for efficient bit-slice software implementation). It is illustrated in Appendix D.1. In the rest of this report, all the differential path examples in E'_d follow the description given in Appendix D.1.

9.3 Differential attack on JH

Using the methods developed above, we can analyze the strength of JH against differential attacks.

9.3.1 Finding the minimum number of active Sboxes in E_d

As stated in Sect. 9.2.1, for $d \in \{2, 3, 4\}$, we exhaustively searched for the minimum number of active Sboxes. The minimum number of active Sboxes for $2d+1$ Sbox layers is 10, 20, 38 for $d = 2, 3, 4$, respectively. The differential path examples of E'_3 and E'_4 are given in Appendix D.2 and D.3, respectively.

For $d > 4$, we use the methods given in Sect. 9.2 to find the minimum number of active Sboxes. For $2d + 1$ Sbox layers, the minimum number of active Sbox is 64, 112, 176, 296 for $d = 5, 6, 7, 8$. *We conjecture that the minimum number of active Sboxes for* $2d+1$ *Sbox layers can be approximated*

as at least $(2d+1) \times 2^{d/2}$. It indicates that the minimum number of active Sboxes does increase significantly as the value of d increases. The differential path examples of E_5', E_6', E_7' and E_8' are given in Appendix D.4, D.5, D.6 and D.7 respectively.

For E_8, we found that the minimum number of active Sboxes for 42 Sbox layers is 720, as illustrated in the example in Appendix D.8. If we assume that there are 2^{42} multiple paths for a given input/output difference pair, there are still around 700 effective active Sboxes. The large number of active Sboxes shows that JH is strong against the differential collision attack.

9.3.2 Effect of correlated active elements in differential attack

In the differential cryptanalysis of JH, each differential characteristic of an Sbox has a probability of at most $\frac{1}{4}$. Each active Sbox may contribute 2^{-2} to the overall differential probability if the active SBoxes are assumed to be independent. However, when there is correlation between active elements, the overall differential probability may increase.

For the 8-bit-to-8-bit super Sbox (concept from Rijmen and Daemen) consisting of two nonlinear layers (4 Sboxes connected by L), a differential characteristic has a maximum probability of $\frac{12}{256} = 2^{-4.41}$. If we consider that there are 16 combinations of those 4 Sboxes, then the average of those 16 maximum differential probabilities is $\frac{10.875}{256} = 2^{-4.56}$. If only 3 Sboxes are active, then the maximum differential probability is $\frac{10}{256} = 2^{-4.68}$. For the 16-bit-to-16-bit super Sbox consisting of three nonlinear layers, there are 4096 combinations of those 12 Sboxes. If there is only one active Sbox in the first or last Sbox layer, then there are 7 active Sboxes being involved; the maximum differential probability is $\frac{44}{2^{16}} = 2^{-10.54}$, and the average of those 4096 maximum differential probabilities is $2^{-10.98}$. When the minimum number of active Sboxes occurs, we are mainly dealing the 8-bit-to-8-bit super Sbox with 3 active Sboxes, and the 16-bit-to-16-bit super Sbox with 7 active Sboxes. In these situations, we see that the effective differential characteristic of an active Sbox is less than $2^{-1.5}$ (but larger than 2^{-2}).

If we consider that each active Sbox contributes $2^{-1.5}$ to the overall differential probability, then the probability of a differential characteristic involving 700 active Sboxes is about 2^{-1050}.

9.3.3 Differential collision attack and message modification

To study the collision resistance of JH, we conservatively assume that an attacker can efficiently eliminate 16 rounds of E_8 with message modification, then there are 26 Sbox layers being left. (Here we assume that in the message modification, the average computational cost of obtaining a desired differential pair after 16 rounds is the computing cost of one compression function.) For 26 Sbox layers of E_8, we found that a differential charac-

teristic involves at least 432 active Sboxes, as illustrated in the example in Appendix D.9. If we assume that there are 2^{26} multiple paths that a particular input difference results in a particular output difference, then the differential probability is about $2^{-1.5\times 432}\times 2^{26} = 2^{-622}$. We thus expect that a differential collision attack can not succeed with less than 2^{256} operations.

9.3.4 Second-preimage and preimage differential attacks

The differential probability in the compression function is around 2^{-1050}. Since this probability is much smaller than 2^{-512}, we expect that JH is strong against the second-preimage attack.

For the preimage attack on JH, a differential path needs to pass through at least two compression functions due to message padding (one more block is padded to the message before generating message digest). Thus differential preimage attack is more difficult than differential second-preimage attack. JH is expected to be secure against the differential preimage attack.

9.4 Truncated differential cryptanalysis [15]

Truncated differential attack is found to be more powerful against JH than differential attack. In the truncated differential attack on JH, we consider whether an element is active or not instead of the exact value of the difference. Let us consider those four Sboxes connected by a linear transformation L. If only one of two Sboxes before L is active, then both Sboxes after L are active with probability 1. We call this event as active element expansion. If both two Sboxes before L are active and independent, then the probability that only one Sbox after L is active is 2^{-4}. We call this event as active element shrinking. If there are b independent active elements after the last round, then the probability that this difference is cancelled by the message difference (if there is message difference at those locations) is 2^{-4b}. For a truncated differential characteristic, we count the number of active element shrinking events and the number of active Sboxes in the last Sbox layer of E_8, and denote the sum of these two numbers as TD_8.

9.4.1 Truncated differential collision attack

Exploiting the symmetry property of E_8, we found in our analysis that the smallest value of TD_8 is 232, as illustrated in the example in Appendix D.8. If we assume that the message modification can effectively remove 16 rounds in the truncated differential collision attack, then the smallest value of TD_8 is 136, as illustrated in the example in Appendix D.9. Assume that there are 2^{26} multiple paths, it requires around $2^{136\times 4-26} = 2^{518}$ trials to generate a collision. (Here we assume that in the message modification, the average computational cost of obtaining a desired differential pair after 16 rounds is the computing cost of one compression function.) Since 2^{518} is much larger

than the complexity of brute force (2^{256}), we consider that JH is strong against the truncated differential collision attack.

9.4.2 Truncated differential (second) preimage attack

In the above analysis, the smallest value of TD_8 is 232. It means that the probability that a truncated differential pair results in a collision is at most 2^{-928}. Since this probability is much smaller than 2^{-512}, we expect that JH is strong against the second-preimage attack.

For the preimage attack on JH, a differential path needs to pass through at least two compression functions due to message padding (one more block is padded to the message before generating message digest). Thus truncated differential preimage attack is more difficult than truncated differential second-preimage attack. JH is expected to be secure against the truncated differential preimage attack.

9.5 Algebraic attacks

Algebraic attacks solve the nonlinear equations in order to recover the key or message. For hash function cryptanalysis, algebraic attacks may be applied to find collision, second preimage and preimage if the algebraic equations of the compression function are very weak.

In the past several years, algebraic attacks have been proposed against block ciphers, but so far there is no evidence that algebraic attacks can break a practical block cipher faster than statistical cryptanalysis techniques, and there is no evidence that the complexity of algebraic attacks against block ciphers would be linear to the round number. The new cube attacks [10] can solve nonlinear equations with low degree, or with high degree but highly non-random equations, when a number of equations (involve the same secret key) are available.

To be conservative, we use constant bits to select Sboxes to further strengthen JH against algebraic attacks. Two 4×4-bit Sboxes are used in JH. Each bit of a 256-bit round constant selects which Sbox is used. Such selection is to increase the overall algebraic complexity. The algebraic degree of each Sbox (and its inverse) is 3.

To find a collision of JH with algebraic attack, the meet-in-the-middle approach results in algebraic equations of 21 Sbox layers. To find a second-preimage with algebraic attack, two blocks of message must be considered, and thus an algebraic attack needs to deal with algebraic equations of 42 Sbox layers. Recovering a message from the message digest would involve at least 36 Sbox layers since one more block is padded to the message. Since the algebraic degree of the Sbox is 3 and the number of rounds being involved is large (at least 21 rounds), we consider that JH is secure against the known algebraic attacks.

9.6 Security of the JH compression function structure

The simple JH compression function structure reduces the cost of security evaluation with respect to differential cryptanalysis. As shown in Sect. 9.3, the JH compression function is secure against differential attack as long as the bijective function being used is strong (there is sufficient confusion and diffusion after message modification).

In the following, we study the security of the JH compression structure with respect to other attacks instead of differential attack. Let E denote a $2m$-bit bijective function (permutation) in the compression function. Denote $H^{(i)} = H^{(i)}_{left} \| H^{(i)}_{right}$. $M^{(i)}$, $H^{(i)}_{left}$ and $H^{(i)}_{right}$ are m-bit. The message digest size is m-bit.

Pseudo-collision (-preimage and -second primage) resistance. The compression function of JH is reversible for a given message, so it is trivial to get pseudo-collision (-preimage and -second preimage) of the JH compression structure, as pointed out by Nasour Bagheri at the NIST mailing list.

However this type of attack (pseudo-collision, etc.) is not a threat to the JH compression function structure since in applications, the $2m$-bit initial value of $H^{(0)}$ is fixed. In the design of JH, we have taken into consideration the reversible property of the compression function, so we use 1024-bit hash value for JH-512 so as to resist the meet-in-the-middle (second) preimage attack.

The trivial pseudo-collision (-preimage -second preimage) has no effect on the security of JH structure and sponge structure as long as the hash value size is large enough. But pseudo-collision is a serious threat to some other types of structures, such as the Davies-Meyer structure. (For the Davies-Meyer structure, a pseudo-collision found through differential attack reveals serious differential weakness in the compression function, and the chance is there that the attack can be improved to find collision.) So whether pseudo-collision is important or not highly depends on the compression function structure being used, and the attack being used.

Collision resistance. If differential attack is not used to find collision, then for a difference in $M^{(i)}$, even finding collision of $H^{(i)}_{right}$ already requires $2^{m/2}$ operations. It thus takes at least $2^{m/2}$ operations to find a collision.

Preimage resistance. If differential attack is not used to find preimage attack, the direct approach is the brute force attack that requires 2^m operations. Another attack is the meet-in-the-middle approach that tries to find a collision of a hash value – an attacker tries to find a collision at $H^{(i)}$. However, the complexity of this approach is significantly higher than the direct brute force attack since it requires the collision search over the space of 2^{2m}, and it takes 2^m operations and 2^m memories.

Mendel and Thomsen have tried to reduced the complexity of the meet-in-the-middle attack through finding multicollisions of half of a hash value [19]. In their attack, the computational cost is reduced to $2^{510.3}$ with $2^{510.6}$ memory, and the number of memory access is increased to 2^{524} [28]. Their attack is much more expensive than the direct brute force attack that requires only 2^{512} computations and almost no memory. So the security of JH is not affected by their attack. The meet-in-the-middle attack was further improved by Bhattacharyya et al. [3]. Their attack finds a preimage with 2^{507} computations and 2^{507} memory, but their attack requires about 2^{526} memory accesses.

Second preimage resistance. The second preimage meet-in-the-middle attack is the same as the preimage meet-in-the-middle attack, and the security of JH is not affected.

9.7 Rebound attack

Rebound attack [18] is a powerful tool to analyze a compression function. The advantage of rebound attack is that it can maximize the effect of "message modification". However, for most of the hash functions that are not using Matyas-Meyer-Oseas-like compression function structure, it would be difficult to develop a rebound attack into a collision attack.

Rijmen et al. have applied rebound attack to analyze the compression function of JH, and it was shown that semi-free-start collision attack can be applied to 16 rounds of JH (with 2^{178} computations and 2^{101} memory, and semi-free-start near collision attack can be applied to 22 rounds of JH (with 2^{156} computations and 2^{143} memory) [21]. Naya-Plasencia showed very recently that the computational complexity and memory complexity of the attacks can be reduced to around 2^{95}.

9.8 Security of padding and final truncation

At least 512 bits are padded to the message so as the ensure that at least one compression function is computed after the last bit of the message, then the message digest is truncated from the output from the last compression function.

If the last bit of $M^{(N-1)}$ is '1', then it is possible to introduce difference only to the last block M^N since the message size can be either $512 \times (N-1)$ or $512 \times (N-1) - 1$. Now if there is collision for H^N_{right}, then there is collision for the message digest. And if there is non-randomness in H^N_{right}, then the message digest is nonrandom. However, the security of JH would not be affected since there is no message modification in the last message block, thus it is difficult to generate collision or nonrandomness for H^N_{right} (the message digest).

If the last bit of $M^{(N-1)}$ is '1', then it is possible to introduce difference only to the last block M^N since the message size can be either $512 \times (N-1)$ or $512 \times (N-1) - 1$. Now suppose that there is difference in $H^{(N-1)}$ such that $\Delta H^{(N-1)} = \Delta M^{(N)}$, then there is no differential propagation in the bijective function in the last compression function, and the message digest difference would be $\Delta M^{(N)}$. However, it is rather difficult to generate $\Delta H^{(N-1)}$ to satisfy $\Delta H^{(N-1)} = \Delta M^{(N)}$ since the size of $H^{(N-1)}$ is $2m$-bit and there is only one choice for $\Delta M^{(N)} \neq 0$. So the security of JH would not be affected.

10 Performance of JH

JH can be implemented efficiently on a wide range of platforms: from hardware to 128-bit/256-bit instructions. The reason is that the generalized AES design allows JH being constructed from extremely simple elements. The 5-bit-to-4-bit (including the constant bit) Sbox can be implemented with 20 binary operations (including ANDNOT operation), the linear transformation L can be implemented with 10 binary operations, and up to 256 Sboxes can be computed in parallel. The simple components and high parallelizability ensure that JH is hardware and software efficient.

10.1 Hardware

The hardware implementation of JH is simple and efficient due to the simple Sboxes and linear transformation. JH uses 1024-bit memory for storing the state of E_8, 512-bit memory for storing the message block, and 256-bit memory to store a round constant (if the round constants are generated on-the-fly).

We compare JH with the ultra-lightweight block cipher PRESENT [7]. The hardware complexity of JH is comparable to that of PRESENT, except for the difference in block sizes. JH uses slightly more complicated Sboxes and linear transformation than PRESENT. The block size of E_8 is about 16 times that of PRESENT, while the size of a round constant in E_8 is only 4 times that of key size of PRESENT. A rough estimation is that E_8 requires 16 times more gates than PRESENT. PRESENT uses about 1570 GE (gate equivalents), so JH may require $1570 \times 16 \approx 25$K GE (estimated).

There would be tradeoff for the hardware implementation of JH. To reduce the number of gates, only two Sboxes and one MDS code need to be implemented. We expect that various optimized hardware implementations of JH would be developed in the final round of the competition, due to the reduced number of candidates.

10.2 8-bit processor

JH can be implemented on 8-bit processor in two approaches. One approach is to implement the hardware description of JH with table lookup for 5×4-bit Sboxes. The advantage of this approach is that the constant bits can be generated on-the-fly efficiently and it requires very small memory. Another approach is to implement the bit-slice description of JH. With 1152-byte precomputed round constants being stored in ROM, this implementation is expected to be quite fast. Given that the SSE2 bit-slice implementation of JH runs at 16.8 cycles/byte on CORE 2 processor, we can roughly estimate the speed of JH on 8-bit processor. The register size of 8-bit processor is 16 times smaller than that of SSE2 register. If we estimate that the number of instructions being processed per clock cycle on 8-bit processor is 5 times less than that on CORE 2 processor, the speed of the bit-slice implementation of JH on 8-bit processor is about $16 \times 5 \times 16.8 = 1344$ cycles/byte (estimated).

10.3 Intel Core 2 microprocessor

The bit-slice implementation of JH is tested on the latest Intel Core 2 mobile processor T6600 2.2 GHz. (for each core, 32 KB L1 data cache and 32 KB L1 instruction cache). The operating systems are 32-bit and 64-bit Ubuntu 10.04. The compiler being used is the Intel C++ compiler 11.1.

The hash speed is measured by hashing a 256-byte buffer for 2^{24} times (message length is 2^{32} bytes), and using 'startclock()' and 'finishclock()' to measure the hash duration. The hash speed is 19.6 clock cycles/byte with the 64-bit Vista (with optimization option -O2); and it is 23.3 clock cycles/byte on the 32-bit Ubuntu (with optimization option -O3).

JH on 64-bit platform is faster than that on 32-bit platform. The reason is that there are sixteen 128-bit XMM registers on the 64-bit platform of Core 2 processor; while there are only eight 128-bit XMM registers on the 32-bit platform of Core 2 processor.

11 Design Rationale

JH was designed to achieve the following goals:

1. Simple
2. Secure
3. Low-cost security evaluation (differential property can be analyzed relatively easily)
4. Efficient in hardware

5. Efficient in software (especially utilizing the power of 128-bit and 256-bit instructions)

6. Avoid table lookup in the fast software implementation

If we avoid using table lookup in the fast software implementation, *the challenge is to design the diffusion components that can be computed efficiently in software, and its diffusion property (security) can be evaluated easily.* Eventually, we use the MDS code over multi-dimensional array for diffusion in JH. The MDS code can be analyzed relatively easily due to the regular diffusion pattern, and the use of multidimensional array allows us to develop and test attacks on low dimensional arrays. (Another major diffusion approach is to use irregular diffusion pattern, such as irregular shifts. The security evaluation cost of that approach is high.)

11.1 Compression function F_d

The construction of compression function F_d from bijective function E_d is new. It gives an extremely simple and efficient approach to construct a compression function from a bijective function (a large block cipher with constant key).

In F_d, the message block size is half of the block size of E_d. The message is XORed with the first half of the input to E_d, then it is XORed with the second half of the output from E_d to achieve one-wayness (for message). Besides the one-wayness, this construction is very efficient – every bit in the output from E_d is not truncated; and the difference cancellation involving the message is minimized. The message block size is only half of the block size of E_d, it is to prevent copying a collision block to other locations, and it is also helpful to resist attacks launched from the middle of E_d.

In the hash function, at least one more block is appended to the message. It is to randomize the final hash value before truncation.

11.2 The generalized AES design methodology

The generalized AES design methodology (Sect. 2.2) being used to construct the bijective function E_d is simple and efficient. The input to E_d is grouped into a d-dimensional array. The nonlinear layer consists of Sboxes. In the linear layer of the r-th round, MDS code is applied along the $(r \bmod d)$-th dimension of the array.

The generalized AES design is easy to analyze due to its symmetrical construction. Round constants are applied to prevent the symmetry property being exploited in attacks.

The generalized AES design is efficient in hardware since E_d can be built upon small components and its round functions are identical. The general-

ized AES design is also efficient in software since it can be implemented in a bit-slice approach.

11.3 Round number

The round number of E_8 is $6 \times (8 - 1) = 42$. The round number is chosen to satisfy two requirements. One requirement is that the round number is the multiple of $d - 1$ so that the hardware description is simple since at the end of the multiple of $d - 1$ rounds, the output from the hardware description is identical to that from the bit-slice implementation. Another requirement is that the round number should be larger than $5d$ in order to build a conservative design. We thus set the round number of E_8 as 42.

The round number 42 is used for all the JH algorithms for two reasons – one reason is to achieve the simplicity of description and implementation; another reason is to achieve extremely large security margin for JH-256 (JH-224), and it also eliminates the threat of multicollision attack against JH-224 and JH-256.

In the original design, the round number is set to 35.5 rounds. The half round is not efficient for hardware implementation since additional circuits are needed to implement it. By changing the round number to 42, we can re-use the same round function in hardware implementation, and we can also obtain larger security margin. (Frank K. Gurkaynak has mentioned the problem of the last half round of AES in the NIST hash forum in 2010.)

11.4 Selecting SBoxes

Two Sboxes are used in JH. Each round constant bit selects which Sboxes are used. Similar design has been used in Feistel's block cipher Lucifer [12] in which a key bit selects which Sboxes are used. The main reason that we use two different Sboxes selected by round constant bits is to increase the complexity of the system algebraic equations so that JH can have better resistance against the future algebraic attack.

11.5 SBoxes

We list eight security requirements for the Sboxes, then give an approach to construct the Sboxes efficiently.

11.5.1 Security requirements

The 4×4-bit Sboxes S_0 and S_1 are designed to meet the following requirements:

1. There is no identical point for two Sboxes, i.e., for the same input, the outputs from two different Sboxes are different.

2. Each differential characteristic has a probability of at most $\frac{1}{4}$.

3. Each linear characteristic [16] has a probability in the range $\frac{1}{2} \pm \frac{1}{4}$.

4. The nonlinear order of each output bit as a function of the input bits is 3.

5. The algebraic normal forms of the two Sboxes are different. (Especially, some degree-3 monomials should appear in some algebraic normal forms of $S_0 \oplus S_1$.)

6. The resulting super Sboxes (formed with more than one Sbox layer, introduced by Rijmen and Daemen, mainly to address the effect of correlated active elements) are strong against differential cryptanalysis.

Note that we do not enforce an input difference with one-bit weight results in an output difference with at least two-bit weight. The reason is that the linear transformation in JH is implemented as MDS code, instead of bit-wise permutation.

Putting two Sboxes together, we have a 5×4-bit Sbox with one input bit being the round constant bit that selects which Sboxes are used. This Sbox satisfies the following requirements:

7. Each differential characteristic has a probability of at most $\frac{1}{4}$.

8. Each linear characteristic has a probability in the range $\frac{1}{2} \pm \frac{1}{4}$.

11.5.2 Constructing SBoxes

The direct approach for constructing the Sboxes is to design two independent Sboxes, then to select one of them using a constant bit. This approach is excellent in security since the algebraic difference between these two Sboxes can be maximized. However, such approach requires too many computations. To reduce computational cost, we construct two dependent Sboxes. This approach gives tradeoff between computational cost and the algebraic difference between those two Sboxes. Thus we can generate efficiently two Sboxes with certain algebraic difference between them.

We search through a lot of circuits, then select the circuit that results in the desired Sboxes. To search for the circuit corresponding to two 4×4-bit Sboxes, the following 11 steps are used (as shown in Sect. 7.2.1). In the first step, one bit of the input is XORed to '1' to ensure that the input 'zero' gets transformed. In the second step, the constant bit is multiplied with another bit so as to alter the circuit. In the third step, a feedforward bit 't' is generated to contain information of the constant bit and three input bits. Step 4 to Step 9 are the invertible nonlinear functions that update the input.

Step 10 and Step 11 use the feedforward bit 't' to alter the output so as to increase the algebraic complexity, and to increase the algebraic difference between those two Sboxes. Note that Step 10 and Step 11 are noninvertible.

We use the following options to generate a lot of circuits: from Step 2 to Step 10, every nonlinear operation can be set as one of two operations (AND, OR); and each operand of the nonlinear operation can be set as itself or its inverse. Thus there are about 2^{27} possible circuits. These circuits correspond to a lot of Sboxes, but most of the Sboxes are noninvertible. We then search for the Sboxes that satisfy the above eight requirements.

The 5×4-bit Sbox being used in JH can be implemented with 20 binary operations (AND, ANDNOT, XOR, NOT, OR), as given in Sect. 7.2.1. The resulting Sboxes achieve good tradeoff between computational cost and the algebraic difference between those two Sboxes. There are three degree-3 monomials in those 4 algebraic normal forms of $S_0 \oplus S_1$. We expect that such algebraic difference is sufficient for increasing the algebraic complexity of the compression function. The algebraic normal forms of S_0, S_1 and $S_0 \oplus S_1$ are given in Appendix C.1, C.2, C.3, respectively. The algebraic normal forms of their inverse are given in Appendix C.4, C.5 and C.6, respectively.

11.6 Linear transform

The linear transform L is probably the simplest (4,2,3) MDS code over $GF(2^4)$. It requires only ten XOR operations. We can compute 128-bit codes efficiently using the 128-bit SIMD/SSE instructions. Furthermore, changing the MDS computation from one dimension to another dimension can also be performed easily, and it requires at most 20 SIMD/SSE instructions, as illustrated in the JH bitslice implementation in Sect. 7.3.

If we use (8,4,5) MDS code over $GF(2^4)$ and use 128-bit instructions, the computational cost of a diffusion layer (MDS code and the changing of dimension) is at least three times of that used in JH. It is the reason that we use the (4,2,3) MDS code over $GF(2^4)$ in the design of JH.

12 Advantages and Limitations

JH hash algorithms have the following advantages:

1. Simple design. The overall design is very simple due to the simple compression function structure and the generalized design methodology. (The hardware and software descriptions are different so as to achieve efficient hardware and software implementations. But it takes some efforts to work out the relations between the hardware and software descriptions).

2. The JH compression function structure gives a simple and efficient approach to construct a compression function from a bijective function

(a block cipher with constant key). This structure is proposed to improve the computational efficiency of sponge structure so that there is no truncation of the output from the bijective function.

3. The generalized AES design methodology gives a simple way to construct a large block cipher from small components by increasing the dimension number.

4. Security analysis can be performed relatively easily. Three approaches are used to achieve this goal. The first approach is to avoid introducing extra variables into the middle of the compression function so that the differential propagation can be analyzed relatively easily. The second approach is to use the generalized AES design methodology that can greatly simplify the differential cryptanalysis. The third approach is that the generalized AES design involves a multidimensional array, so the array with low dimension can be easily studied to estimate the strength of the high dimensional array.

5. High efficiency for collision resistance. The generalized AES design methodology would likely maximize the difference propagation. The JH compression function is likely to minimize the difference cancellation within a compression function.

6. JH can be implemented efficiently on hardware and 128-bit/256-bit processors (SIMD/SSE2/AVX instructions). The reason is that the generalized AES design allows JH being built from extremely simple components.

   (a) Hardware efficient. The hardware description of JH is simple. The internal state size of E_8 is only 1024 bits and the message block size is 512 bits. The round constants can be generated on the fly with 256-bit additional memory. Both the Sboxes and linear transformation in JH are extremely simple.

   (b) Software efficient. JH is designed to exploit the computational power of modern and widely used microprocessors. The bitslice description of E_8 can be efficiently implemented with the SIMD/SSE2/AVX instructions.

7. Several variants are available by varying the parameter d. The extremely hardware-efficient F_6 (increasing the round number to 30) is suitable for achieving about 128-bit security for collision resistance, preimage resistance and second-preimage resistance for a message with length less than 2^{64} bits. For this tiny hash function, the hash size is 256 bits, the message block size is 128 bits, the message digest size is 256 bits.

8. It is convenient to use JH to substitute SHA2 [20] in almost all the SHA2 applications.

Although JH can be used directly to construct a message authentication code (MAC) (such as HMAC), the resulting MAC is not that efficient. In general, constructing a MAC from a strong hash function is not that efficient since the secret key in MAC can significantly reduce computational cost. We think that a dedicated efficient MAC standard is needed since MAC is used extensively in secure data communication, and the performance of MAC is critical for high speed or hardware constrained applications.

13 Conclusion

In this document, we proposed JH hash algorithms which are both hardware and software efficient. Our analysis shows that JH is very secure. However, the extensive security analysis of any new design requires a lot of efforts from many researchers. We thus invite and encourage researchers to analyze the security of JH. JH is not covered by any patent and JH is freely-available.

Acknowledgement

Part of the design was done when the author was studying at the research group COSIC of the Katholieke Universiteit Leuven. I would like to thank Paul Crowley for independently implementing JH, detecting the bug in my original JH code and suggesting the formula for computing the number of zero bits being padded to the message. I would like to thank Tomasz Anuszkiewicz, Thomas Pornin and Wenling Wu for their comments on the bugs in the code and report. And I would like to thank Frank K. Gurkaynak and Bernhard Jungk for their comments on the last half round of AES/JH. And I would like to thank Prof Bart Preneel for the discussion on the round number. I would also like to thank Donghoon Chang for pointing out the unclear parts in my report, and thank Souradyuti Paul for the discussion on compression function structure. Finally, I would like to thank all the researchers who have implemented and analyzed JH in the last two years.

References

[1] R. Anderson, E. Biham and L. Knudsen. "SERPENT: A Flexible Block Cipher with Maximum Assurance." The first AES candidate conference, 1998.

[2] G. Bertoni, J. Daemen, M. Peeters and G. Van Assche, "Sponge Functions." ECRYPT hash workshop 2007.

[3] R. Bhattacharyya, A. Mandal, M. Nandi. "Security Analysis of the Mode of JH Hash Function." Fast Software Encryption – FSE 2010, pp. 168–191.

[4] E. Biham, A. Shamir, "Differential Cryptanalysis of DES-like Cryptosystems." *Advances in Cryptology – Crypto'90*, LNCS 537, pp. 2-21, Springer-Verlag, 1991.

[5] E. Biham, R. Chen, "Near-Collisions of SHA-0." *Advances in Cryptology – CRYPTO 2004*, pp. 290–305, Springer-Verlag, 2004.

[6] E. Biham, R. Chen, A. Joux, P. Carribault, C. Lemuet, W. Jalby, "Collisions of SHA-0 and Reduced SHA–1." *Advances in Cryptology – EUROCRYPT 2005*, pp. 36–57, Springer-Verlag, 2005.

[7] A. Bogdanov, L. R. Knudsen, G. Leander, C. Paar, A. Poschmann, M. J. B. Robshaw, Y. Seurin and C. Vikkelsoe, "PRESENT: An Ultra-Lightweight Block Cipher ." *Cryptographic Hardware and Embedded Systems – CHES 2007*, pp. 450–466, Springer-Verlag, 2007.

[8] F. Chabaud, A. Joux, "Differential Collisions in SHA-0." *Advances in Cryptology – CRYPTO 1998*, pp. 56-71, Springer-Verlag, 1998.

[9] J. Daeman and V. Rijmen, "AES Proposal: Rijndael." Available on-line from NIST at http://csrc.nist.gov/encryption/aes/rijndael/

[10] I. Dinur and A. Shamir, "Cube Attacks on Tweakable Black Box Polynomials." IACR ePrint, 2008. Available at http://eprint.iacr.org/2008/385

[11] H. Dobbertin, "Cryptanalysis of MD4." *Fast Software Encryption – FSE 1996*, pp. 53–69, Springer-Verlag, 1996.

[12] H. Feistel, "Cryptography and Computer Privacy." Scientific American, vol.228(5), May 1973, pp 15–23.

[13] A. Joux, T. Peyrin. "Hash Functions and the (Amplified) Boomerang Attack." Advances in Cryptology – CRYPTO 2007, pp. 244–263.

[14] J. Kelsey, T. Kohno, "Herding Hash Functions and the Nostradamus Attack." *Advances in Cryptology – EUROCRYPT 2006*, pp. 183–200, Springer-Verlag, 2006.

[15] L. Knudsen, "Truncated and Higher Order Differentials." *Fast Software Encryption – FSE'94*, pp. 196–211, Springer-Verlag.

[16] M. Matsui, "Linear Cryptanalysis Method for DES Cipher." *Advances in Cryptology – Eurocrypt'93*, LNCS 765, pp. 386-397, Springer-Verlag, 1994.

[17] S.M. Matyas, C.H. Meyer and J. Oseas, "Generating strong one-way functions with cryptographic algorithm." IBM Technical Disclosure Bulletin, 27 (1985), 5658–5659.

[18] F. Mendel, C. Rechberger, M. Schlaffer, and S. S. Thomsen. "The Rebound Attack: Cryptanalysis of Reduced Whirlpool and Grostl." Fast Software Encryption – FSE 2009, pp. 260–276.

[19] F. Mendel, S. S. Thomsen. "An Observation on JH-512." Ecrypt hash website. http://ehash.iaik.tugraz.at/uploads/d/da/Jh_preimage.pdf

[20] National Institute of Standards and Technology, "Secure Hash Standard (SHS)." Available at http://csrc.nist.gov/cryptval/shs.html

[21] V. Rijmen, D. Toz, K. Varici. "Rebound Attack on Reduced-Round Versions of JH." Fast Software Encryption – FSE 2010, pp. 286–303.

[22] J. Stern, S. Vaudenay. "CS-Cipher." *Fast Software Encryption – FSE'98*, pp. 189–205, Springer-Verlag, 1998.

[23] X. Wang, X. Lai, D. Feng, H. Chen, X. Yu, "Cryptanalysis of the Hash Functions MD4 and RIPEMD." *Advances in Cryptology – EUROCRYPT 2005*, pp. 1–18, Springer-Verlag, 2005.

[24] X. Wang, H. Yu, "How to Break MD5 and Other Hash Functions." *Advances in Cryptology – EUROCRYPT 2005*, pp. 19–35, Springer-Verlag, 2005.

[25] X. Wang, H. Yu, Y. L. Yin, "Efficient Collision Search Attacks on SHA-0." *Advances in Cryptology – CRYPTO 2005*, pp. 1–16, Springer-Verlag, 2005.

[26] X. Wang, Y. L. Yin, H. Yu, "Finding Collisions in the Full SHA-1." *Advances in Cryptology – CRYPTO 2005*, pp. 17–36, Springer-Verlag, 2005.

[27] R. Winternitz. "A secure one-way hash function built from DES." IEEE Symposium on Information Security and Privacy, p. 88–90, 1984.

[28] H. Wu. "The Complexity of Mendel and Thomsen's Preimage Attack on JH-512." Ecrypt website. http://ehash.iaik.tugraz.at/uploads/6/6f/Jh_mt_complexity.pdf

A Round constants of E_8

This section gives the round constants in E_8. E_8 has 42 256-bit round constants.

A.1 Round constants in the hardware implementation of E_8

The round constants are generated from the first round constant using round function R_6 (with the round constants of R_6 being set to 0).

```
C00 = 6a09e667f3bcc908b2fb1366ea957d3e
      3adec17512775099da2f590b0667322a
C01 = bb896bf05955abcd5281828d66e7d99a
      c4203494f89bf12817deb43288712231
C02 = 1836e76b12d79c55118a1139d2417df5
      2a2021225ff6350063d88e5f1f91631c
C03 = 263085a7000fa9c3317c6ca8ab65f7a7
      713cf4201060ce886af855a90d6a4eed
C04 = 1cebafd51a156aeb62a11fb3be2e14f6
      0b7e48de85814270fd62e97614d7b441
C05 = e5564cb574f7e09c75e2e244929e9549
      279ab224a28e445d57185e7d7a09fdc1
C06 = 5820f0f0d764cff3a5552a5e41a82b9e
      ff6ee0aa615773bb07e8603424c3cf8a
C07 = b126fb741733c5bfcef6f43a62e8e570
      6a26656028aa897ec1ea4616ce8fd510
C08 = dbf0de32bca77254bb4f562581a3bc99
      1cf94f225652c27f14eae958ae6aa616
C09 = e6113be617f45f3de53cff03919a94c3
      2c927b093ac8f23b47f7189aadb9bc67
C10 = 80d0d26052ca45d593ab5fb310250639
      0083afb5ffe107dacfcba7dbe601a12b
C11 = 43af1c76126714dfa950c368787c81ae
      3beecf956c85c962086ae16e40ebb0b4
C12 = 9aee8994d2d74a5cdb7b1ef294eed5c1
      520724dd8ed58c92d3f0e174b0c32045
C13 = 0b2aa58ceb3bdb9e1eef66b376e0c565
      d5d8fe7bacb8da866f859ac521f3d571
C14 = 7a1523ef3d970a3a9b0b4d610e02749d
      37b8d57c1885fe4206a7f338e8356866
C15 = 2c2db8f7876685f2cd9a2e0ddb64c9d5
      bf13905371fc39e0fa86e1477234a297
C16 = 9df085eb2544ebf62b50686a71e6e828
      dfed9dbe0b106c9452ceddff3d138990
C17 = e6e5c42cb2d460c9d6e4791a1681bb2e
      222e54558eb78d5244e217d1bfcf5058
C18 = 8f1f57e44e126210f00763ff57da208a
      5093b8ff7947534a4c260a17642f72b2
C19 = ae4ef4792ea148608cf116cb2bff66e8
      fc74811266cd641112cd17801ed38b59
```

```
C20 = 91a744efbf68b192d0549b608bdb3191
      fc12a0e83543cec5f882250b244f78e4
C21 = 4b5d27d3368f9c17d4b2a2b216c7e74e
      7714d2cc03e1e44588cd9936de74357c
C22 = 0ea17cafb8286131bda9e3757b3610aa
      3f77a6d0575053fc926eea7e237df289
C23 = 848af9f57eb1a616e2c342c8cea528b8
      a95a5d16d9d87be9bb3784d0c351c32b
C24 = c0435cc3654fb85dd9335ba91ac3dbde
      1f85d567d7ad16f9de6e009bca3f95b5
C25 = 927547fe5e5e45e2fe99f1651ea1cbf0
      97dc3a3d40ddd21cee260543c288ec6b
C26 = c117a3770d3a34469d50dfa7db020300
      d306a365374fa828c8b780ee1b9d7a34
C27 = 8ff2178ae2dbe5e872fac789a34bc228
      debf54a882743caad14f3a550fdbe68f
C28 = abd06c52ed58ff091205d0f627574c8c
      bc1fe7cf79210f5a2286f6e23a27efa0
C29 = 631f4acb8d3ca4253e301849f157571d
      3211b6c1045347befb7c77df3c6ca7bd
C30 = ae88f2342c23344590be2014fab4f179
      fd4bf7c90db14fa4018fcce689d2127b
C31 = 93b89385546d71379fe41c39bc602e8b
      7c8b2f78ee914d1f0af0d437a189a8a4
C32 = 1d1e036abeef3f44848cd76ef6baa889
      fcec56cd7967eb909a464bfc23c72435
C33 = a8e4ede4c5fe5e88d4fb192e0a0821e9
      35ba145bbfc59c2508282755a5df53a5
C34 = 8e4e37a3b970f079ae9d22a499a714c8
      75760273f74a9398995d32c05027d810
C35 = 61cfa42792f93b9fde36eb163e978709
      fafa7616ec3c7dad0135806c3d91a21b
C36 = f037c5d91623288b7d0302c1b941b726
      76a943b372659dcd7d6ef408a11b40c0
C37 = 2a306354ca3ea90b0e97eaebcea0a6d7
      c6522399e885c613de824922c892c490
C38 = 3ca6cdd788a5bdc5ef2dceeb16bca31e
      0a0d2c7e9921b6f71d33e25dd2f3cf53
C39 = f72578721db56bf8f49538b0ae6ea470
      c2fb1339dd26333f135f7def45376ec0
C40 = e449a03eab359e34095f8b4b55cd7ac7
      c0ec6510f2c4cc79fa6b1fee6b18c59e
C41 = 73bd6978c59f2b219449b36770fb313f
      be2da28f6b04275f071a1b193dde2072
```

A.2 Round constants in the bit-slice implementation of E_8

Each round constant used in the bit-slice implementation of E_8 is linked to the corresponding round constant in the hardware implementation through a permutation.

```
C'00_even = 72d5dea2df15f8677b84150ab7231557
C'00_odd  = 81abd6904d5a87f64e9f4fc5c3d12b40
C'01_even = ea983ae05c45fa9c03c5d29966b2999a
C'01_odd  = 660296b4f2bb538ab556141a88dba231
C'02_even = 03a35a5c9a190edb403fb20a87c14410
C'02_odd  = 1c051980849e951d6f33ebad5ee7cddc
C'03_even = 10ba139202bf6b41dc786515f7bb27d0
C'03_odd  = 0a2c813937aa78503f1abfd2410091d3
C'04_even = 422d5a0df6cc7e90dd629f9c92c097ce
C'04_odd  = 185ca70bc72b44acd1df65d663c6fc23
C'05_even = 976e6c039ee0b81a2105457e446ceca8
C'05_odd  = eef103bb5d8e61fafd9697b294838197
C'06_even = 4a8e8537db03302f2a678d2dfb9f6a95
C'06_odd  = 8afe7381f8b8696c8ac77246c07f4214
C'07_even = c5f4158fbdc75ec475446fa78f11bb80
C'07_odd  = 52de75b7aee488bc82b8001e98a6a3f4
C'08_even = 8ef48f33a9a36315aa5f5624d5b7f989
C'08_odd  = b6f1ed207c5ae0fd36cae95a06422c36
C'09_even = ce2935434efe983d533af974739a4ba7
C'09_odd  = d0f51f596f4e81860e9dad81afd85a9f
C'10_even = a7050667ee34626a8b0b28be6eb91727
C'10_odd  = 47740726c680103fe0a07e6fc67e487b
C'11_even = 0d550aa54af8a4c091e3e79f978ef19e
C'11_odd  = 8676728150608dd47e9e5a41f3e5b062
C'12_even = fc9f1fec4054207ae3e41a00cef4c984
C'12_odd  = 4fd794f59dfa95d8552e7e1124c354a5
C'13_even = 5bdf7228bdfe6e2878f57fe20fa5c4b2
C'13_odd  = 05897cefee49d32e447e9385eb28597f
C'14_even = 705f6937b324314a5e8628f11dd6e465
C'14_odd  = c71b770451b920e774fe43e823d4878a
C'15_even = 7d29e8a3927694f2ddcb7a099b30d9c1
C'15_odd  = 1d1b30fb5bdc1be0da24494ff29c82bf
C'16_even = a4e7ba31b470bfff0d324405def8bc48
C'16_odd  = 3baefc3253bbd339459fc3c1e0298ba0
C'17_even = e5c905fdf7ae090f947034124290f134
C'17_odd  = a271b701e344ed95e93b8e364f2f984a
C'18_even = 88401d63a06cf61547c1444b8752afff
C'18_odd  = 7ebb4af1e20ac6304670b6c5cc6e8ce6
C'19_even = a4d5a456bd4fca00da9d844bc83e18ae
```

```
C'19_odd  = 7357ce453064d1ade8a6ce68145c2567
C'20_even = a3da8cf2cb0ee11633e906589a94999a
C'20_odd  = 1f60b220c26f847bd1ceac7fa0d18518
C'21_even = 32595ba18ddd19d3509a1cc0aaa5b446
C'21_odd  = 9f3d6367e4046bbaf6ca19ab0b56ee7e
C'22_even = 1fb179eaa9282174e9bdf7353b3651ee
C'22_odd  = 1d57ac5a7550d3763a46c2fea37d7001
C'23_even = f735c1af98a4d84278edec209e6b6779
C'23_odd  = 41836315ea3adba8fac33b4d32832c83
C'24_even = a7403b1f1c2747f35940f034b72d769a
C'24_odd  = e73e4e6cd2214ffdb8fd8d39dc5759ef
C'25_even = 8d9b0c492b49ebda5ba2d74968f3700d
C'25_odd  = 7d3baed07a8d5584f5a5e9f0e4f88e65
C'26_even = a0b8a2f436103b530ca8079e753eec5a
C'26_odd  = 9168949256e8884f5bb05c55f8babc4c
C'27_even = e3bb3b99f387947b75daf4d6726b1c5d
C'27_odd  = 64aeac28dc34b36d6c34a550b828db71
C'28_even = f861e2f2108d512ae3db643359dd75fc
C'28_odd  = 1cacbcf143ce3fa267bbd13c02e843b0
C'29_even = 330a5bca8829a1757f34194db416535c
C'29_odd  = 923b94c30e794d1e797475d7b6eeaf3f
C'30_even = eaa8d4f7be1a39215cf47e094c232751
C'30_odd  = 26a32453ba323cd244a3174a6da6d5ad
C'31_even = b51d3ea6aff2c90883593d98916b3c56
C'31_odd  = 4cf87ca17286604d46e23ecc086ec7f6
C'32_even = 2f9833b3b1bc765e2bd666a5efc4e62a
C'32_odd  = 06f4b6e8bec1d43674ee8215bcef2163
C'33_even = fdc14e0df453c969a77d5ac406585826
C'33_odd  = 7ec1141606e0fa167e90af3d28639d3f
C'34_even = d2c9f2e3009bd20c5faace30b7d40c30
C'34_odd  = 742a5116f2e032980deb30d8e3cef89a
C'35_even = 4bc59e7bb5f17992ff51e66e048668d3
C'35_odd  = 9b234d57e6966731cce6a6f3170a7505
C'36_even = b17681d913326cce3c175284f805a262
C'36_odd  = f42bcbb378471547ff46548223936a48
C'37_even = 38df58074e5e6565f2fc7c89fc86508e
C'37_odd  = 31702e44d00bca86f04009a23078474e
C'38_even = 65a0ee39d1f73883f75ee937e42c3abd
C'38_odd  = 2197b2260113f86fa344edd1ef9fdee7
C'39_even = 8ba0df15762592d93c85f7f612dc42be
C'39_odd  = d8a7ec7cab27b07e538d7ddaaa3ea8de
C'40_even = aa25ce93bd0269d85af643fd1a7308f9
C'40_odd  = c05fefda174a19a5974d66334cfd216a
C'41_even = 35b49831db411570ea1e0fbbedcd549b
```

```
C'41_odd  = 9ad063a151974072f6759dbf91476fe2
```

B Developing the Bit-Slice Implementation of JH

The description of JH given in Sect. 4 and Sect. 5 are suitable for efficient hardware implementation. In this section, we illustrate the bit-slice implementation of JH. The bit-slice implementation of F_d uses $d-1$ different round function descriptions (the hardware description of F_d uses identical round function description).

B.1 Bit-slice parameters

The following additional parameters are used in the bit-slice implementation of JH.

$C_r'^{(d)}$	The round constant words used in the bit-slice implementation of E_d with $0 \le r \le 5 \times (d-1)$. Each $C_r'^{(d)}$ is a 2^d-bit constant word.
$C_{r,even}'^{(d)}$	Even bits of $C_r'^{(d)}$. $C_{r,even}'^{(d)} = C_r'^{(d),0} \parallel C_r'^{(d),2} \parallel C_r'^{(d),4} \parallel \cdots \parallel C_r'^{(d),2^d-2}$. Each $C_{r,even}'^{(d)}$ is a 2^{d-1}-bit constant word.
$C_{r,odd}'^{(d)}$	Odd bits of $C_r'^{(d)}$. $C_{r,odd}'^{(d)} = C_r'^{(d),1} \parallel C_r'^{(d),3} \parallel C_r'^{(d),5} \parallel \cdots \parallel C_r'^{(d),2^d-1}$. Each $C_{r,odd}'^{(d)}$ is a 2^{d-1}-bit constant word.
$H_j^{(i)}$	The j^{th} 128-bit word of the i^{th} hash value. $H_0^{(i)}$ is the left-most 128-bit word of hash value $H^{(i)}$.
$M_j^{(i)}$	The j^{th} 128-bit word of the i^{th} message block. $M_0^{(i)}$ is the left-most word of message block $M^{(i)}$.

B.2 Bit-slice functions

The following functions are used in the bit-slice implementation of JH.

B.2.1 Sboxes

S^{bitsli} implements both S_0 and S_1 in the bit-slice implementation of JH. Let each x_i ($0 \le i \le 3$) denotes a 2^{d-1}-bit word. Let c denote a 2^{d-1}-bit constant word, t denote a temporary word. $(x_0, x_1, x_2, x_3) = S^{bitsli}(x_0, x_1, x_2, x_3, c)$ is computed in the following 11 steps (x_3 are the least significant bits):

1. $x_3 = \neg x_3$;
2. $x_0 = x_0 \oplus (c \,\&\, (\neg x_2))$;
3. $t = c \oplus (x_0 \,\&\, x_1)$;
4. $x_0 = x_0 \oplus (x_2 \,\&\, x_3)$;
5. $x_3 = x_3 \oplus ((\neg x_1) \,\&\, x_2)$;
6. $x_1 = x_1 \oplus (x_0 \,\&\, x_2)$;
7. $x_2 = x_2 \oplus (x_0 \,\&\, (\neg x_3))$;
8. $x_0 = x_0 \oplus (x_1 | x_3)$;
9. $x_3 = x_3 \oplus (x_1 \,\&\, x_2)$;
10. $x_1 = x_1 \oplus (t \,\&\, x_0)$;
11. $x_2 = x_2 \oplus t$;

B.2.2 Linear Transform

L^{bitsli} implements the linear transform in the bit-slice implementation of JH. Let each a_i and b_i $(0 \leq i \leq 7)$ denotes a 2^{d-1}-bit word. $(b_0, b_1, \cdots, b_7) = L^{bitsli}(a_0, a_1, \cdots, a_7)$ is computed as follows:

$$\begin{aligned}
b_4 &= a_4 \oplus a_1\,; \qquad b_5 = a_5 \oplus a_2\,; \\
b_6 &= a_6 \oplus a_3 \oplus a_0\,; \; b_7 = a_7 \oplus a_0\,; \\
b_0 &= a_0 \oplus b_5\,; \qquad b_1 = a_1 \oplus b_6\,; \\
b_2 &= a_2 \oplus b_7 \oplus b_4\,; \; b_3 = a_3 \oplus b_4\,.
\end{aligned}$$

B.2.3 Permutation $\bar{\omega}$

Let $A = (a_0, a_1, \cdots, a_{2\times\alpha\times n-1})$, where α and n are positive integers. Let $B = (b_0, b_1, \cdots, b_{2\times\alpha\times n-1})$. Each a_i and b_i denotes a 4-bit element. The permutation $B = \bar{\omega}(A, n)$ is computed as follows:

$$\begin{aligned}
&\text{for } i = 0 \text{ to } \alpha - 1\,, \\
&\quad \text{for } j = 0 \text{ to } n - 1\,, \\
&\qquad b_{2\times i\times n+j} = a_{2\times i\times n+n+j}\,;\; b_{2\times i\times n+n+j} = a_{2\times i\times n+j}\,;
\end{aligned}$$

For example, $\bar{\omega}(A, 1)$ swaps element a_{2i} and a_{2i+1}.

B.2.4 Permutation ω

Permutation $\omega(A, n)$ swaps the bits in a word A. It is computed by treating each bit in A as an element, then applying the permutation $\bar{\omega}(A, n)$.

B.2.5 Permutation $\bar{\sigma}_d$

Permutation $\bar{\sigma}_d$ operates on 2^d elements. Let $A = (a_0 \parallel a_1 \parallel \cdots \parallel a_{2^d-1})$, $B = (b_0 \parallel b_1 \parallel \cdots \parallel b_{2^d-1})$. Let $n = 2^\beta$, where β is an integer smaller than $d - 1$. $B = \bar{\sigma}_d(A, n)$ permutes the odd elements in A as follows:

$$\begin{aligned}
(b_1, b_3, b_5, \cdots, b_{2^d-1}) &= \bar{\omega}((a_1, a_3, a_5, \cdots, a_{2^d-1})\,, n)\,; \\
(b_0, b_2, b_4, \cdots, b_{2^d-2}) &= (a_0, a_2, a_4, \cdots, a_{2^d-2})\,.
\end{aligned}$$

B.2.6 Permutation σ_d

Permutation $\sigma_d(A, n)$ operates on the bits in a word A. It is computed by treating each bit in A as an element, then applying the permutation $\bar{\sigma_d}(A, n)$.

B.2.7 Round constants

Let IP_d denote the inverse of P_d. Let IP_d^r denote the composition of r permutation IP_d :

$$IP_d^r = \underbrace{IP_d \circ IP_d \circ \cdots \circ IP_d}_{r} .$$

Note that IP_d^r has the property that $IP_d^r = IP_d^{r+\alpha \cdot d}$.

Let permutation $\lambda_d^r(A)$ operate on the bits in a word A. It is computed by treating each bit in A as an element, then applying the permutation IP_d^r.

Let η_d^r denote a permutation. Let A, B and V_i denote 2^d-bit words. $B = \eta_d^r(A)$ is computed as follows:

$V_0 = A$;
for $i = 0$ to $r-1$, $\quad V_{i+1} = \sigma_d(V_i, 2^{i \bmod (d-1)})$;
$B = V_r$;

The round constant $C_r'^{(d)}$ is generated from $C_r^{(d)}$ as:

$$C_r'^{(d)} = \eta_d^r \circ \lambda_d^r(C_r^{(d)}) .$$

The 2^{d-1}-bit constant words $C_{r,even}'^{(d)}$ and $C_{r,odd}'^{(d)}$ are obtained by extracting the even and odd bits of $C_r'^{(d)}$, respectively, as defined in Appendix B.1. $C_{r,even}'^{(8)}$ and $C_{r,odd}'^{(8)}$ are given in Appendix A.2.

B.2.8 An alternative description of round function R_d

The description of R_d in Sect. 4.4 is suitable for hardware implementation. But that description is not suitable for the bit-slice implementation. We give here an alternative description of R_d, and denote the r-th round function as $R'_{d,r}$. The 2^d-bit round constant of the r-th round is denoted as $C_r'^{(d)}$. Let $V = v_0 \parallel v_1 \parallel \cdots \parallel v_{2^d-1}$, where each v_i denotes a 4-bit word. The computation of $B = R'_{d,r}(A, C_r'^{(d)})$ is given as follows:

1. for $i = 0$ to $2^d - 1$,
   {
   if $C_r'^{(d),i} = 0$, then $v_i = S_0(a_i)$;
   if $C_r'^{(d),i} = 1$, then $v_i = S_1(a_i)$;
   }
2. $(v_{2i}, v_{2i+1}) = L(v_{2i}, v_{2i+1})$ $\quad$ for $0 \le i \le 2^{d-1} - 1$;
3. $B = \bar{\sigma}_d(V,\, 2^{r \bmod (d-1)})$

Note that $R'_{d,r}$ has the following properties:

1. The description of $R'_{d,r}$ is the same as $R'_{d,r+\alpha\cdot(d-1)}$ except for the different round constants.

2. For the same input passing through multiple rounds, at the end of the $\alpha\cdot(d-1)$-th round, the output from $R'_{d,\alpha\cdot(d-1)}$ is identical to the output from $R_{d,\alpha\cdot(d-1)}$.

Six rounds of $R'_{4,r}$ $(0 \le r \le 5)$ are illustrated in Fig. 11.

B.2.9 Bit-slice implementation of round function R_d

The above description of $R'_{d,r}$ can be implemented efficiently in a bit-slice way. The method used is to separate the odd and even elements of A in $R'_{d,r}$. Denote the bit-slice implementation as $R^{bitsli}_{d,r}$. Let A and B represent two 2^{d+2}-bit words, $A = a_0 \,\|\, a_1 \,\|\, a_2 \,\|\, \cdots \,\|\, a_7$, and $B = b_0 \,\|\, b_1 \,\|\, b_2 \,\|\, \cdots \,\|\, b_7$, where each A_i and B_i represents a 2^{d-1}-bit word. Let each v_i and u_i $(0 \le i \le 7)$ denote a 2^{d-1}-bit word. The computation of $B = R^{bitsli}_{d,r}(A, C'^{(d)}_{r,even}, C'^{(d)}_{r,odd})$ is given as follows:

1. $(v_0, v_2, v_4, v_6) = S^{bitsli}(a_0, a_2, a_4, a_6, C'^{(d)}_{r,even})$;
   $(v_1, v_3, v_5, v_7) = S^{bitsli}(a_1, a_3, a_5, a_7, C'^{(d)}_{r,odd})$;

2. $(u_0, u_2, u_4, u_6, u_1, u_3, u_5, u_7) = L^{bitsli}(v_0, v_2, v_4, v_6, v_1, v_3, v_5, v_7)$;

3. $b_0 = u_0$; $b_2 = u_2$; $b_4 = u_4$; $b_6 = u_6$;
   $b_1 = \omega(u_1,\, 2^{r \bmod (d-1)})$;
   $b_3 = \omega(u_3,\, 2^{r \bmod (d-1)})$;
   $b_5 = \omega(u_5,\, 2^{r \bmod (d-1)})$;
   $b_7 = \omega(u_7,\, 2^{r \bmod (d-1)})$;

B.2.10 Bit-slice implementation of E_d

The 2^{d+2}-bit input and output are denoted as A and B, respectively. Let each Q_r denote a 2^{d+2}-bit word for $0 \le r \le 6(d-1)$. The computation of $B = E_d(A)$ is given as follows:

1. $Q_0 = A$;

2. for $r = 0$ to $6(d-1)-1$, $\quad Q_{r+1} = R^{bitsli}_{d,r}(Q_r, C'^{(d)}_{r,even}, C'^{(d)}_{r,odd})$;

The generation of the round constants is given in Appendix B.2.7.

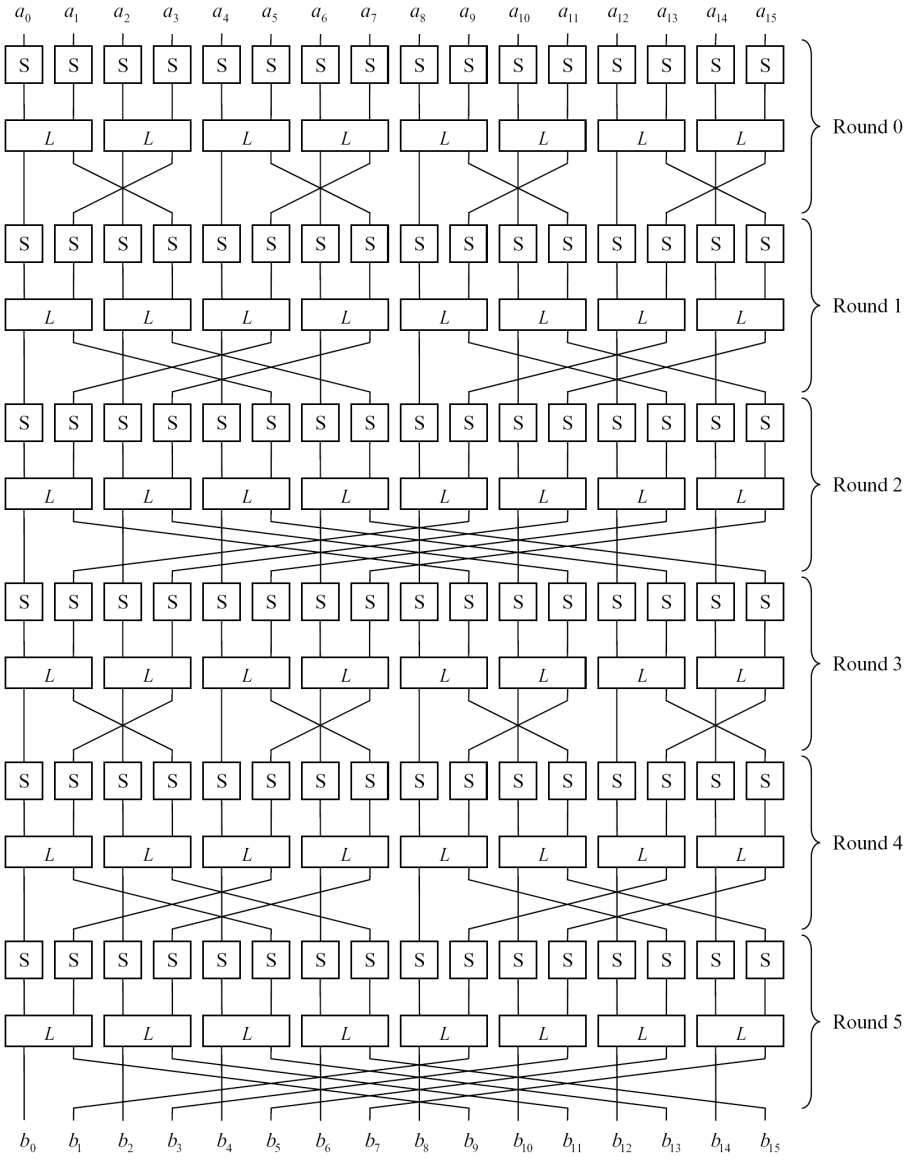

Figure 11: An alternative description of 6 rounds of R_4(constant bits not shown)

C Algebraic Normal Forms of Sboxes

This section gives the algebraic normal forms of S_0, S_1 and $S_0 \oplus S_1$. The input to an Sbox is denoted as $x = x0\|x1\|x2\|x3$, and the output of an Sbox is denoted as $y = y0\|y1\|y2\|y3$.

C.1 Algebraic normal forms of S_0

```
y3 = 1 + x3 + x2 + x2x1 + x3x2x1 + x3x2x0 + x3x1x0 + x2x1x0
y2 = x3x2 + x2x1 + x3x0 + x2x0 + x1x0 + x3x2x1 + x2x1x0
y1 = x2 + x3x2 + x1 + x2x0 + x2x1x0
y0 = 1 + x3 + x2 + x0 + x3x1 + x2x0 + x3x2x1 + x3x2x0 + x2x1x0
```

Monomial with degree 3 appears in all the four expressions. And monomial with degree 3 appears in any linear combination of the above four expressions.

C.2 Algebraic normal forms of S_1

```
y3 = 1 + x3 + x2 + x3x1 + x2x1 + x3x2x0 + x3x1x0 + x2x1x0
y2 = 1 + x3 + x1 + x3x0 + x2x0 + x1x0 + x3x2x1 + x2x1x0
y1 = x3 + x2 + x1 + x0 + x3x2 + x3x1 + x3x2x1 + x3x2x0
y0 = x3 + x0 + x3x1 + x2x0 + x3x2x1 + x3x2x0 + x2x1x0
```

Monomial with degree 3 appears in all the four expressions. And monomial with degree 3 appears in any linear combination of the above four expressions.

C.3 Algebraic normal forms of $S_0 \oplus S_1$

```
y3 = x3x1 + x3x2x1
y2 = 1 + x3 + x1 + x3x2 + x2x1
y1 = x3 + x0 + x3x1 + x2x0 + x3x2x1 + x3x2x0 + x2x1x0
y0 = 1 + x2
```

Note that the algebraic normal forms of $S_0 \oplus S_1$ are not random. It is due to tradeoff between the computational cost and the algebraic difference between S_0 and S_1. We expect that such algebraic difference between S_0 and S_1 is sufficient for increasing the algebraic complexity of the overall compression function.

C.4 Algebraic normal forms of S_0^{-1}

```
y3 = 1 + x3 + x2 + x1 + x0 + x3x2 + x3x2x1 + x3x0
     + x3x2x0 + x3x1x0 + x2x1x0
y2 = x2 + x1 + x0 + x3x1 + x2x1 + x3x0 + x2x1x0
y1 = x0 + x3x2 + x3x1 + x3x0 + x2x0 + x3x2x1 + x2x1x0
y0 = x3 + x2 + x0 + x2x0 + x1x0 + x3x2x1 + x3x1x0 + x2x1x0
```

Monomial with degree 3 appears in all the four expressions. And monomial with degree 3 appears in any linear combination of the above four expressions.

C.5 Algebraic normal forms of S_1^{-1}

```
y3 = x2 + x1 + x0 + x3x2 + x3x1 + x2x0 + x1x0
     + x3x2x1 + x3x1x0 + x2x1x0
y2 = 1 + x2 + x3x1 + x2x1 + x1x0 + x2x1x0
y1 = x3 + x0 + x3x2 + x3x0 + x1x0 + x3x2x1 + x3x2x0 + x2x1x0
y0 = 1 + x3 + x2x1 + x1x0 + x3x2x1 + x3x2x0 + x3x1x0
```

Monomial with degree 3 appears in all the four expressions. And monomial with degree 3 appears in any linear combination of the above four expressions.

C.6 Algebraic normal forms of $S_0^{-1} \oplus S_1^{-1}$

```
y3 = 1 + x3 + x3x1 + x3x0 + x2x0 + x1x0 + x3x2x0
y2 = 1 + x1 + x0 + x3x0 + x1x0
y1 = x3 + x3x1 + x2x0 + x1x0 + x3x2x0
y0 = 1 + x2 + x0 + x2x1 + x2x0 + x3x2x0 + x2x1x0
```

Note that the algebraic normal forms of $S_0^{-1} \oplus S_1^{-1}$ are not random. It is due to tradeoff between the computational cost and the algebraic difference between S_0^{-1} and S_1^{-1}. We expect that such algebraic difference between S_0^{-1} and S_1^{-1} is sufficient for increasing the algebraic complexity of the overall compression function.

D Differential path examples

In our differential and truncated differential attacks, we used the following description of E'_d to find the minimum probability of differential path (for convenience). The differential path example given in this section all follow the description given in Appendix D.1.

D.1 An alternative description of E'_d

E'_d in Sect. 9.2.2 can be described in an alternative form (the form that can be used for efficient bit-slice software implementation). Denote the r-th round function as $R''_{d,r}$. The 2^d-bit round constant of the r-th round is denoted as $C_r''^{(d)}$. Let $V = v_0 \| v_1 \| \cdots \| v_{2^d-1}$, where each v_i denotes a 4-bit word. The computation of $B = R''_{d,r}(A, C_r''^{(d)})$ is given as follows:

1. for $i = 0$ to $2^d - 1$,
   {
   if $C_r''^{(d),i} = 0$, then $v_i = S_0(a_i)$;

if $C_r^{\prime\prime(d),i} = 1$, then $v_i = S_1(a_i)$;

}

2. (a) If $r \bmod d = 0$, $(v_{2i}, v_{2i+1}) = L(v_{2i}, v_{2i+1})$ for $0 \le i \le 2^{d-1} - 1$;
   (b) If $r \bmod d = 1$, $(v_{4i}, v_{4i+2}) = L(v_{4i}, v_{4i+2})$,
   $(v_{4i+1}, v_{4i+3}) = L(v_{4i+1}, v_{4i+3})$ for $0 \le i \le 2^{d-2} - 1$;
   (c) If $r \bmod d = 2$, $(v_{8i}, v_{8i+4}) = L(v_{8i}, v_{8i+4})$,
   $(v_{8i+1}, v_{8i+5}) = L(v_{8i+1}, v_{8i+5})$, $(v_{8i+2}, v_{8i+6}) = L(v_{8i+2}, v_{8i+6})$,
   $(v_{8i+3}, v_{8i+7}) = L(v_{8i+3}, v_{8i+7})$ for $0 \le i \le 2^{d-3} - 1$;
   (d) $\cdots\cdots$

Four rounds of E_4' are illustrated in Fig. 12 (after four rounds, the next four rounds would be similar to the previous four rounds, except for the different round constants).

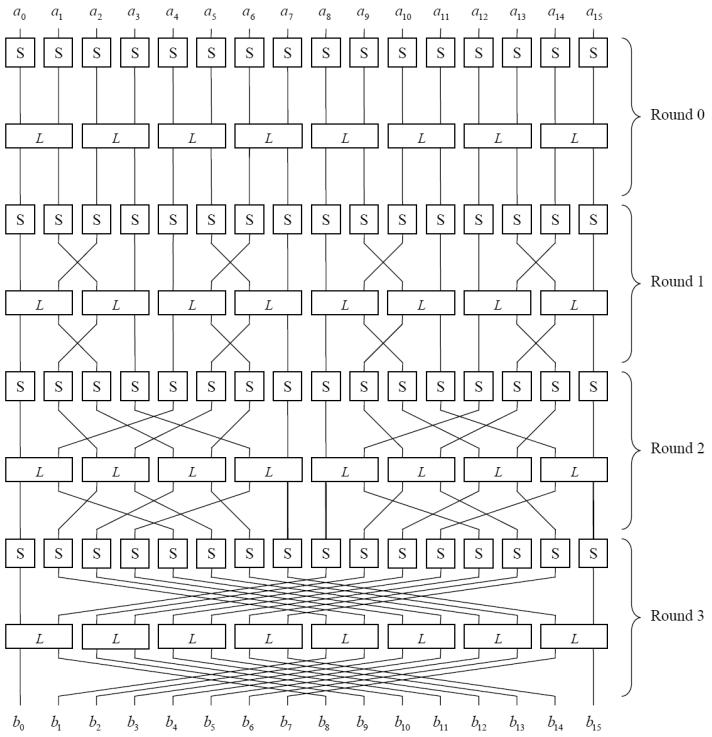

Figure 12: Four rounds in alternative E_4' (round constants are not shown)

D.2 Differential path example of 7 rounds of E_3'

The following differential path involves 20 active Sboxes. There are 7 rows, and each row involves 8 elements. The '*' signs in the i-th row indicate the positions of the active Sboxes in the i-th round.

```
*0*00000
****0000
**000000
**00**00
*000*000
*0*0*0*0
*0*00000
```

D.3 Differential path example of 9 rounds of E'_4

The following differential path involves 38 active Sboxes. There are 9 rows, and each row involves 16 elements. The '*' signs in the i-th row indicate the positions of the active Sboxes in the i-th round.

```
*0*0000000000000
****000000000000
**00000000000000
**00**0000000000
**00**00**00**00
*000*000*000*000
*0*0*0*0*0*0*0*0
*0*00000*0*00000
*0*0000000000000
```

D.4 Differential path example of 11 rounds of E'_5

The following differential path involves 64 active Sboxes. There are 15 rows, and each row involves 32 elements. The '*' signs in the i-th row indicate the positions of the active Sboxes in the i-th round.

```
*0*00000*0*00000000000000000000000
****0000****00000000000000000000000
**000000**00000000000000000000000000
**00**00**00**00000000000000000000000
**00**0000000000000000000000000000000
**00**0000000000**00**0000000000
*000*00000000000*000*00000000000
*0*0*0*000000000*0*0*0*000000000
*0*0000000000000*0*0000000000000
*0*00000*0*00000*0*00000*0*00000
*0*00000*0*00000000000000000000000
```

D.5 Differential path example of 13 rounds of E'_6

The following differential path involves 112 active Sboxes. There are 13 rows, and each row involves 64 elements. The '*' signs in the i-th row indicate the positions of the active Sboxes in the i-th round.

```
*0*00000*0*0000000000000000000000000000000000000000000000000000000000000000
****0000****0000000000000000000000000000000000000000000000000000000000000000
**000000**00000000000000000000000000000000000000000000000000000000000000000000
**00**00**00**00000000000000000000000000000000000000000000000000000000000000000
**00**0000000000000000000000000000000000000000000000000000000000000000000000000
**00**0000000000**00**00000000000000000000000000000000000000000000000000000000
**00**0000000000**00**0000000000**00**0000000000**00**0000000000
*000*00000000000*000*00000000000*000*00000000000*000*00000000000
*0*0*0*000000000*0*0*0*000000000*0*0*0*000000000*0*0*0*000000000
*0*0000000000000*0*0000000000000*0*0000000000000*0*0000000000000
*0*00000*0*00000*0*00000*0*00000*0*00000*0*00000*0*00000*0*00000
*0*00000*0*00000000000000000000*0*00000*0*00000000000000000000
*0*00000*0*0000000000000000000000000000000000000000000000000000000000000000
```

D.6 Differential path example of 15 rounds of E_7'

The following differential path involves 176 active Sboxes. There are 15 rows, and each row involves 128 elements. The '*' signs in the i-th row indicate the positions of the active Sboxes in the i-th round.

D.7 Differential path example of 17 rounds of E_8'

The following differential path involves 296 active Sboxes. There are 17 rows, and each row involves 256 elements. The '*' signs in the i-th row indicate the positions of the active Sboxes in the i-th round.

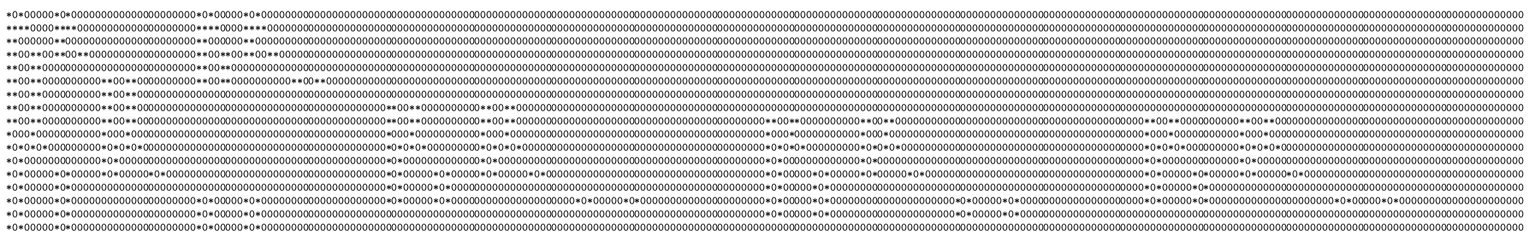

D.8 Differential path example of 42 rounds of E'_8

The following differential path involves 720 active Sboxes. And the value of TD_8 in the truncated differential collision attack is 232. There are 42 rows, and each row involves 256 elements. The '*' signs in the i-th row indicate the positions of the active Sboxes in the i-th round.

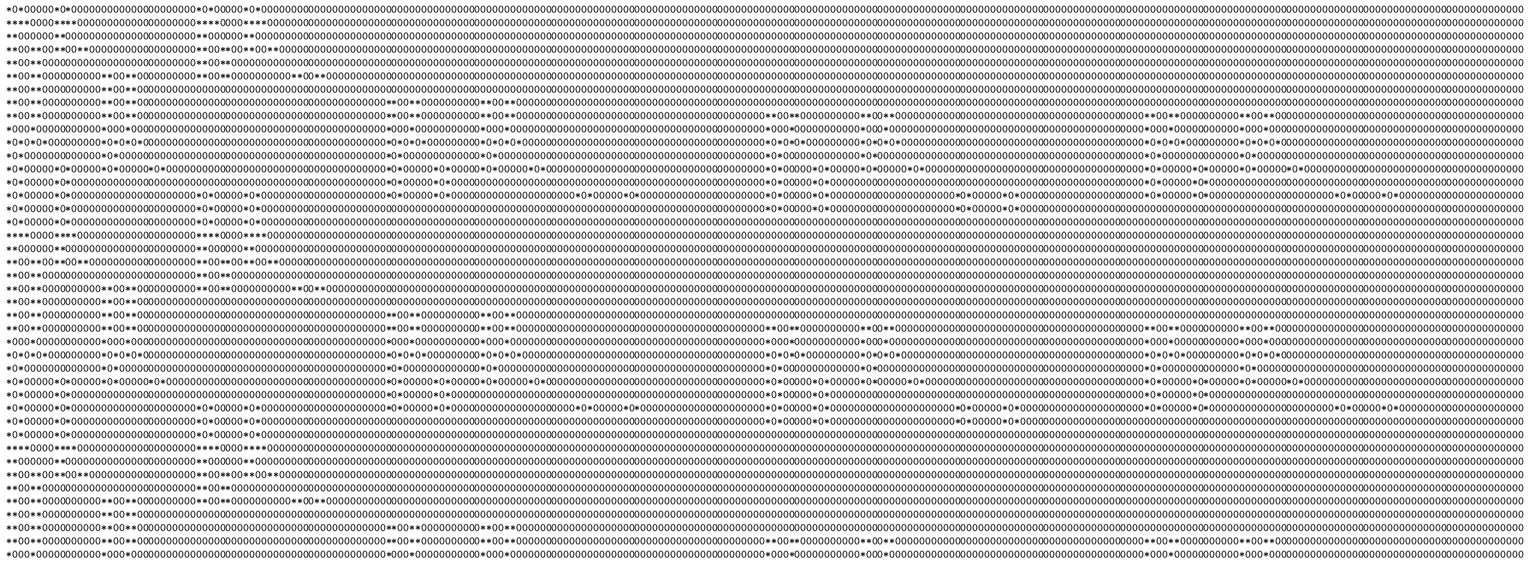

D.9 Differential path example of 26 rounds of E'_8

The following differential path involves 432 active Sboxes. And the value of TD_8 in the truncated differential attack is 136. There are 26 rows, and each row involves 256 elements. The '*' signs in the i-th row indicate the positions of the active Sboxes in the i-th round.